LOW COMPLEXITY SCALABLE BEHAVIORAL MODELING

OF RF POWER AMPLIFIERS WITH MEMORY EFFECTS

BY

ABDEREZAK MIFTAH KEDIR

A Thesis Presented to the

DEANSHIP OF GRADUATE STUDIES

KING FAHD UNIVERSITY OF PETROLEUM & MINERALS

DHAHRAN, SAUDI ARABIA

In Partial Fulfillment of the
Requirements for the Degree of

MASTER OF SCIENCE

In

ELECTRICAL ENGINEERING

December 2013

KING FAHD UNIVERSITY OF PETROLEUM & MINERALS

DHAHRAN- 31261, SAUDI ARABIA

DEANSHIP OF GRADUATE STUDIES

This thesis, written by **Abderezak Miftah Kedir** under the direction his thesis advisor and approved by his thesis committee, has been presented and accepted by the Dean of Graduate Studies, in partial fulfillment of the requirements for the degree of **MASTER OF SCIENCE IN ELECTRICAL ENGINEERING.**
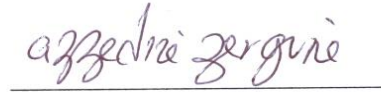
Dr. Oualid Hammi
(Advisor)

Dr. Ali A Al-Shaikhi
Department Chairman

Dr. Azzedine Zerguine
(Member)

Dr. Salam A. Zummo
Dean of Graduate Studies

Dr. Mohammed S. Sharawi
(Member)

26th December, 2013
Date

Dedication

To Mom and Dad

ACKNOWLEDGMENTS

The last but not the least, I would like to give my utmost gratitude to the most important people in my life, my family. I am humbly dedicating this work to my mom, Hadra Ahmed, and my dad, Miftah Kedir, who have given me everything in life by sacrificing theirs! May Allah give me the ability to pay back all their favors in this life and may Allah grant them paradise in the hereafter for raising me in good manners. My mother always used to tell me to get one more degree for her, and another for dad. This is for you mom! And my wife, Zehara Amin, one of the best things happened to me. I would like to thank her for her patience and encouragement during my studies. I want to extend my love and gratitude to her for letting me have her in my life.

I am so happy to see this chapter of my life come to an end. As it is said when one door is closed another will be opened. I am wondering which door will that be.

TABLE OF CONTENTS

LIST OF TABLES

LIST OF FIGURES

X

LIST OF ABBREVIATIONS

DUT	Device Under Test
DC	Direct Current
ETSI	European Telecommunications Standard Institute
FTNTB	Forward Twin Non-linear Two-box
GaN	Gallium Nitride
LDMOS	Laterally Diffused Metal Oxide Semiconductor
LTE	Long Term Evolution
LTI	Linear Time Invariant
LUT	Look-up Table
MP	Memory Polynomial
NMSE	Normalized Mean Square Error
PA	Power Amplifier
PAPR	Peak to Average Power Ratio
RF	Radio Frequency
WCDMA	Wideband Code Division Multiple Access

ABSTRACT

Full Name   : Abderezak Miftah Kedir

Thesis Title   : Low Complexity Scalable Behavioral Modeling of RF Power
                   Amplifiers with Memory Effects

Major Field   : Electrical Engineering

Date of Degree : December 2013

Recent emerging wireless technologies require wider and frequent changes of signal bandwidth. Thus, frequent model size update becomes more necessary in behavioral modeling of power amplifiers that are found in the transmitters of current technologies to keep the accuracy of the model. Moreover due to the use of wider signal bandwidth in recent technologies, the memory effects behavior should be handled as well. To address these issues, a complexity aware metric for the model size selection that takes into account both the complexity in terms of the model size and the system performance in terms of the normalized mean square error (NMSE) is proposed along with a generic bandwidth scalable behavioral model. While the proposed metric is suitable for the selection of the model dimensions in memory polynomial based power amplifiers' behavioral models, the proposed bandwidth scalable model is suitable for addressing the complexity of models of power amplifiers exhibiting memory effects with frequent signal characteristics change. In the proposed bandwidth scalable two-box models, rather than updating the entire model coefficients when the signal bandwidth changes, the memoryless function is maintained unchanged and only the function modeling the dynamic distortions is updated. The model is built around state of the art two-box models, namely the Hammerstein model and the forward twin-nonlinear two-box model. The

proposed model takes advantage of the separation between static and dynamic distortions of the power amplifier. Experimental validations carried on two Doherty power amplifier prototypes illustrate the advantages of the proposed model selection technique as it reduces the model dimension by 60% without compromising its accuracy. The proposed bandwidth scalable models are verified also on two types of power amplifiers and is found to achieve the same performance as the conventional models with considerable reduction in model complexity.

ABSTRACT (ARABIC)

ملخص الرسالة

الاسم الكامل:عبدرزاق مفتاح قدير

عنوان الرسالة: : النمذجة السلوكية قليلة التعقيد المتغيرة لمضخمات الطاقة اللاسلكية مع وجود آثار ذاكرة

التخصص: هندسة كهربائية

تاريخ الدرجة العلمية: : ديسمبر 2013

التقنيات اللاسلكية الحديثة الناشئة تتطلب عرض نطاق ترددى أوسع و متغير بشكل متكرر. و بالتالى فإن التحديث المستمر لحجم الأنموذج السلوكى لمضخمات الطاقة الموجودة فى أجهزة البث اللاسلكية الحديثة بات ضروريا للحفاظ على دقة الأنموذج. بالإضافة إلى ذلك ,فإن استخدام نطاقات تردد أوسع فى التقنيات الحديثة , أدى إلى بروز آثار الذاكرة التى لابد أن تؤخذ أيضا بعين الاعتبار. لمعالجة هذه القضايا, اقترح مقياس تعقيد لاختيار حجم الأنموذج, الذى يأخذ بالاعتبار تعقيد الأنموذج من حيث الحجم, بالإضافة إلى أدائه من حيث الدقة باستخدام مقياس(NMSE). علاوة على ذلك, تم اقتراح أنموذج سلوكى عام متغير على حسب تغير النطاق الترددى للإشارات المرسلة. بينما المقياس المقترح يصلح لاختيار أبعاد الأنموذج فى نماذج الدوال متعددة الحدود لمضخمات الطاقة, فإن الأنموذج المتغير المقترح صالح لمعالجة تعقيد نماذج مضخمات الطاقة التى تظهر آثار الذاكرة مع التغير المستمر لخصائص الإشارات المرسلة. فى نماذج الصندوقين (Two-box models) المتغيرة المقترحة, فبدلا من تحديث معاملات الأنموذج بشكل كامل مع تغير خصائص الإشارات, فإن الدالة عديمة الذاكرة الساكنة تبقى بلا تغيير و فقط يتم تغيير الدالة المسؤولة عن نمذجة السلوك الديناميكى. هذا الأنموذج المقترح تم بناؤه على نسق بناء نماذج الصندوقين المعروفة و المسماة بـ(Hammerstein model) و (the forward twin nonlinear two-box model). الأنموذج المقترح يستفيد من الفصل بين التشوهات الساكنة و التشوهات الديناميكية لمضخمات الطاقة. التأكيدات التجريبية المقامة على مضخمى طاقة من نوع (Doherty) تظهر مميزات أسلوب اختيار الأنموذج المقترح لأنه باستخدام هذا الأسلوب تم تقليل حجم الأنموذج بنسبة (60%) بغير تأثير على دقة الأنموذج. على الجانب الآخر, فإن نماذج النطاقات الترددية

المتغيرة المقترحة قد تم أيضا التحقق منها على مضخمى طاقة مختلفين حيث أظهرت النتائج التجريبية قدرتهم على

الوصول إلى نفس أداء النماذج التقليدية مع انخفاض كبير في درجة التعقيد.

CHAPTER 1

INTRODUCTION

In the last decade, the energy consumption reduction or energy saving technologies have been given focus with main intention to reduce the carbon dioxide (CO_2) emission. The reduction of this emission will contribute to alleviating the global warming problem.

The energy consumption of over millions of wireless transmitter units worldwide are responsible for an appreciable part of the carbon dioxide emission. Based on the European Telecommunications Standard Institute (ETSI) report [1], more than 90% of the energy consumed by wireless communication units goes to the radio units. And from the radio unit, around 50% to 80% of the consumption goes to the power amplifier (PA): around 10% to 25% for air conditioning, 5% to 15% for signal processing and the rest to the power supply units. Efficiency improvement in power amplifiers results a significant reduction of air conditioning power consumption as well. Therefore, improving the efficiency of the PA reduces the power consumption of radio unit since most of the consumption attributes to it. Thus, efficient modeling and linearization of PA is important.

Moreover, the high bandwidth requirement in recent wireless communication standards has a significant impact on the type of PA to be used. A similar impact is eminent on the efficient behavioral modeling and linearization of the PA that is used in the transmitters. Figure 1.1 shows the location of the transmitter in basic communication systems.

1

In the basic communication system presented in Figure 1.1, the signals produced from the source are converted to binary sequences with efficient representation of the source output by the source encoder. The source encoder handles the process of converting the output of the source into a sequence of binary digits. The information sequence or the sequence of binary digits from the source encoder is passed to the channel encoder. The channel encoder introduces some redundancy, in a controlled manner, in the binary information sequence. The controlled redundancies added on the information sequence are useful at the receiver to overcome the noise and interference encountered in the transmission of the signal through the communication channel. Figure 1.1 is simply a basic representation of a communication system some details are deliberately omitted to keep the scope of work.
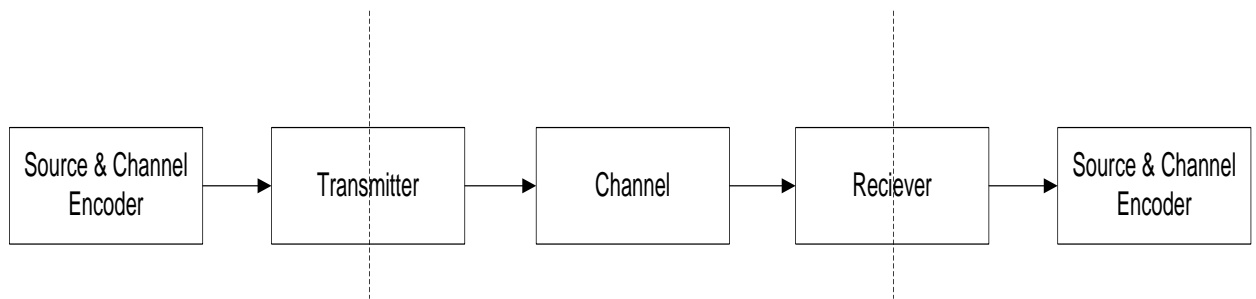
Figure 1.1 Basic communication system

Then, the binary sequence data, or information sequence, will pass through the transmitter. The transmitter consists of the modulator, local oscillator, mixers, filters, isolators, power amplifier and antenna.

The channel, as shown in Figure 1.1, represents the physical medium that is used to send the signal from the transmitter to the receiver. In wireless communication, the physical channel is commonly atmospheric air. The digital demodulator processes the channel corrupted transmitted waveform and reduces it to a sequence that represents estimates of the transmitted data symbols in binary or M-array. This sequence is then passed to the channel decoder, which attempts to reconstruct the original information sequence from knowledge of the code used by the channel encoder and the redundancy contained in the received data.

At the channel decoder output the source decoder reconstructs the original signal that was transmitted from the source. The source decoder does the reconstruction by using the knowledge of the source encoding method used. Finally, the source decoder produces an analogue signal. The difference between the reconstructed and the original signal is a measure of the distortion by the digital communication system. In the next section, general types of signals that are used in communication systems specially the ones that are useful for the power amplifier modeling will be presented.

1.1 Signals in Communication Systems

Signals in communication systems can be categorized as baseband and band-pass signals. The baseband signal has a non-zero value in the vicinity of the origin and negligible value elsewhere in the frequency domain. Conversely the band-pass signal has a non-zero value in the vicinity of the carrier frequency. Modulation is a process of imposing the source information on a band-pass signal by varying its amplitude, frequency, or phase or a combination of these.

Any physical band-pass signal can be represented by

$$x(t) = Re\left[X(t)e^{j\omega_c t}\right] \tag{1}$$

where $X(t)$ is the complex envelope of the band-pass signal, $\omega_c = 2\pi f_c$ and f_c is the carrier frequency.

$x(t)$ can also be represented by other formats. The real and imaginary parts of $X(t)$, $X_I(t)$ and $X_Q(t)$, are called in-phase and quadrature components, respectively,.

$$X(t) = X_I(t) + jX_Q(t) \tag{2}$$

$$X_I(t) = x(t)\cos(\omega_c t) + \hat{x}(t)\sin(\omega_c t) \tag{3}$$

$$X_Q(t) = \hat{x}(t)\cos(\omega_c t) - x(t)\sin(\omega_c t) \tag{4}$$

Where $\hat{x}(t) = \frac{1}{\pi t} * x(t)$ is the Hilbert transform of $x(t)$. The following steps are followed to deduce the equation for the baseband signal equation.

First, the in-phase component will be multiplied by $\cos(\omega_c t)$ and the quadrature component will be multiplied by $\sin(\omega_c t)$ as such

$$X_I(t)\cos(\omega_c t) = x(t)\cos(\omega_c t)\cos(\omega_c t) + \hat{x}(t)\sin(\omega_c t)\cos(\omega_c t) \tag{5}$$

$$X_Q(t)\sin(\omega_c t) = \hat{x}(t)\cos(\omega_c t)\sin(\omega_c t) - x(t)\sin(\omega_c t)\sin(\omega_c t) \tag{6}$$

Equivalently it can rewritten as such

$$X_I(t)\cos(\omega_c t) = x(t)\cos^2(\omega_c t) + \hat{x}(t)\sin(\omega_c t)\cos(\omega_c t) \tag{7}$$

$$X_Q(t)\sin(\omega_c t) = \hat{x}(t)\cos(\omega_c t)\sin(\omega_c t) - x(t)\sin^2(\omega_c t) \tag{8}$$

Subtracting $X_Q(t)\sin(\omega_c t)$ from $X_I(t)\cos(\omega_c t)$ leads to:

$$X_I(t)\cos(\omega_c t) - X_Q(t)\sin(\omega_c t) = x(t)\cos^2(\omega_c t) + x(t)\sin^2(\omega_c t) \tag{9}$$

$$X_I(t)\cos(\omega_c t) - X_Q(t)\sin(\omega_c t) = x(t)(\cos^2(\omega_c t) + \sin^2(\omega_c t)) \tag{10}$$

Since from trigonometry $\cos^2(\omega_c t) + \sin^2(\omega_c t) = 1$

$$X_I(t)\cos(\omega_c t) - X_Q(t)\sin(\omega_c t) = x(t) \tag{11}$$

Thus, the band-pass signal can be represented as follows

$$x(t) = X_I(t)\cos(\omega_c t) - X_Q(t)\sin(\omega_c t) \tag{12}$$

It is also possible to represent the signal $x(t)$ in terms of amplitude modulation $r(t) = |X(t)|$ and phase modulation $\theta(t) = arg(X(t))$.

$$x(t) = r(t)\cos(\omega_c t + \theta(t)) \tag{13}$$

where $r(t)$ and $\theta(t)$ are real baseband signals.

From the above relationship of the complex envelope signal and band-pass signal, the spectrum and power of a band-pass signal and the spectrum and power of its complex envelope signal can be directly related. The spectrum of the band-pass signal can be easily acquired using the frequency translation property of a Fourier transform.

$$x(f) = \frac{1}{2}[X(f - f_c) + X^*(-f - f_c)] \tag{14}$$

Where $x(f)$ and $X(f)$ are Fourier transforms of $x(t)$ and $X(t)$, respectively. The relationship between the power spectral density (PSD) of the band-pass signal and the PSD of the complex envelope signal can be acquired from this. The PSD of $x(t)$ is the Fourier transform of the autocorrelation function of $x(t)$. More details can be found in [2].

The autocorrelation functions of $R_x(\tau)$ and $R_X(\tau)$ can be related as follows:

$$R_x(\tau) = \frac{1}{2} Re[R_X(\tau)e^{j\omega_c\tau}] \tag{15}$$

The baseband signal waveforms with in phase and quadrature components that are presented in this section will be used to model the power amplifiers. In the next section, the nonlinearities of power amplifiers will be discussed.

1.2　Nonlinearity in Power Amplifiers

Most physical systems are nonlinear to some degree; however, it is advantageous to simplify physical systems into linear ones because of the availability of powerful analysis tools for linear systems especially for the linear time invariant (LTI) ones. Moreover, the

6

principle of superposition holds in a linear system however it does not hold for nonlinear systems. In the frequency domain, the output of the linear systems have the same frequency terms as the input signal but in nonlinear systems a number of additional frequency terms appear.

The approximated linear system for the physical system may work well over a limited range of input signal levels. However, in a nonlinear model it is necessary to adequately cover all the ranges of input signal levels. For example in Figure 1.2 the transfer characteristics of a power amplifier is reported. If the input power is small, the PA can be modeled by the linear system but when the input power is large, the nonlinearity in the PA will be significant and the linear system approximation cannot be used.
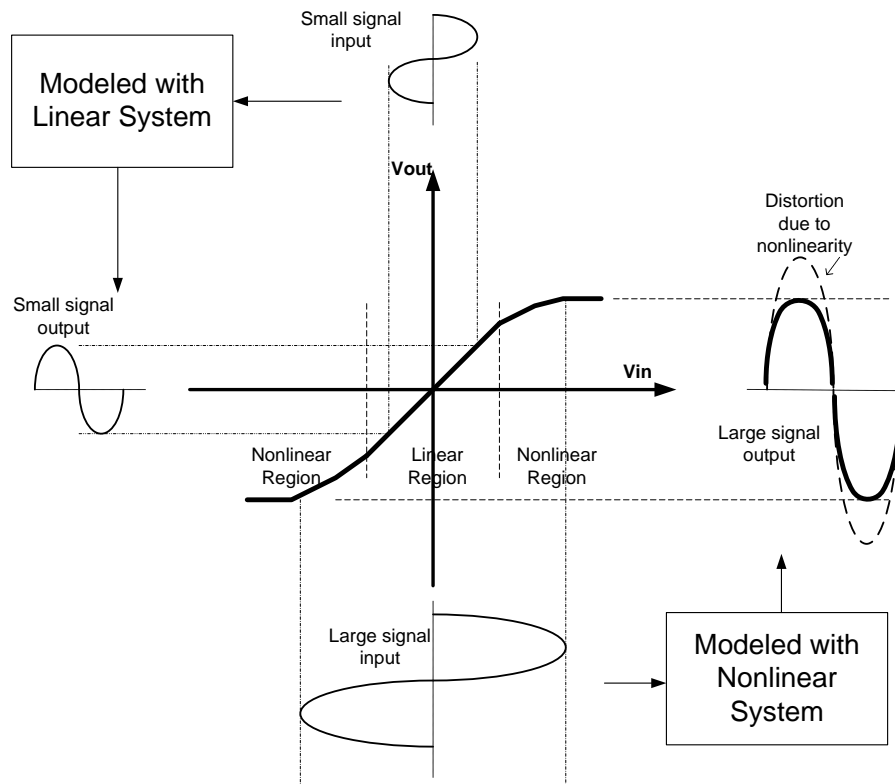
Figure 1.2 Power amplifier's transfer characteristics for small and large signals

7

The nonlinearity that is caused by the radio frequency (RF) PA is due to the operation of the amplifier near the saturation region as shown in Figure 1.3. The y-axis represents the output power of the amplifier in dBm scale and the x-axis represents the input power of the amplifier in dBm. In order to maintain the signal quality, the desired region for the power amplifier is the linear region. However, since the signal has high peak to average power ratio (PAPR), operating the amplifier in the linear region will lead to low average output power and thus low power efficiency. Since it is crucial for an RF PA to have high efficiency, it is commonly operated in the compression region close to saturation to have high efficiency and mild nonlinearity. This nonlinearity caused by operating the amplifier near the saturation region will create distortions and generate intermodulation products. This nonlinearity is typically compensated using linearization techniques. However, to enhance the power efficiency of the power amplifier while operating it up to the saturation region, Doherty power amplifier architecture is widely used in today's wireless transmitters. This architecture will be briefly discussed in section 1.4.

An RF PA is an essential component of the wireless communication system. It has the functionality of increasing the power level of the signal that goes to the antenna to be radiated out. The radiated output signal power may range from 0.2W to 2W for mobile devices and between 10W to 100W for base stations.
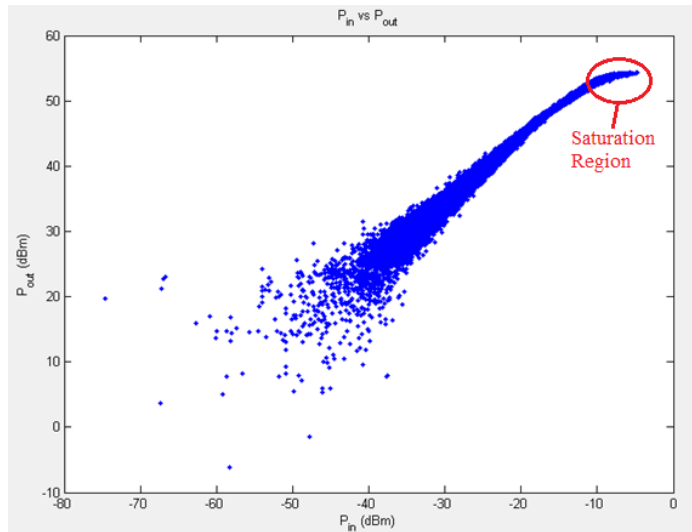
Figure 1.3 Output power vs. input power of a typical power amplifier

When RF PAs are discussed, it is essential to know the type of transistor that has been used with their specific bias type, linearity and efficiency. On the other hand, it is needed to take into account the memory effects of the system as well so that to have better and accurate modeling of the PA when system level analysis is considered.

An RF power amplifier is an amplifier which consists of active circuits that is commonly designed to deliver high output power and efficiency. The technology that is commonly adopted for RF power amplifiers used in wireless communications is the Laterally Diffused Metal Oxide Semiconductor (LDMOS). The LDMOS has very high output power. Although a single LDMOS has a good efficiency, Gallium Nitride (GaN) is able to do better [3]. In cases of signals with high peak to average power ratio used to drive an amplifier, Doherty architecture can be used to increase the efficiency in the 6dB back off region as discussed in [4].

9

A PA can be represented with one block representation as shown in Figure 1.4 . The block representation of PA is very useful in case of system level analysis is considered since it shows a simplified representation with enough information for such analysis.

$x(t)$　$f(.)$　$Y(t)$
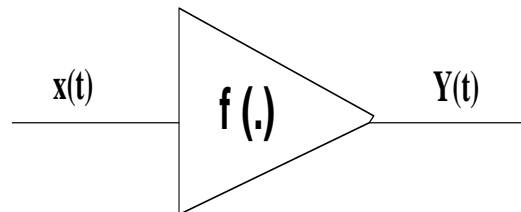
Figure 1.4 PA block representation

The system level analyses of PA mainly focus on the memory effects and the nonlinearity of the system. As the power handling capacity and bandwidth of operation of power amplifiers increase, memory effects become increasingly critical to the performance improvement and behavioral modeling of power amplifiers.

1.3　Memory Effects

One of the most important phenomena to be considered in the behavioral modeling of power amplifiers is the memory effects. A system is said to have memory when it cannot dissipate its energy instantaneously and it stores energy. A PA often shows memory characteristics especially in base stations high power amplifiers. A self-heating effect in the transistor and a long time constant in a DC bias circuit are also one of the reasons for

long term memory effects. However, the memory effects that is going to be discussed in this thesis work is the one that is caused due to the wide bandwidth of the input signal. In such case, it is mainly short term memory effect.

In general, if the actual output of a system is dependent only on its actual input, then that system can be referred to as memoryless. If the output of a system does not only a function of the actual input but also a function of the past input values such that the actual output is influenced by the history of the input signal, then the system is considered with memory. The memory effects of the power amplifier as a system become more severe as the driving signal bandwidth increases. Recent emerging broadband technologies use such wideband signals that could trigger the transmitters to develop memory effects unlike the previous technologies that use narrow band signals for voice applications only.

1.4 Doherty Power Amplifier

The Doherty power amplifier was first proposed in 1936. The main aim of this system was to maintain high efficiency with input signals that have high PAPR in the range of 6 to10 dB. Depending on the manner the transistors are biased, the PA can be classified in several classes, such as classes A, AB, B and C. The Doherty amplifier is a combination of class AB amplifier which has relatively linear characteristics and class C amplifier which is a nonlinear amplifier connected in specific way. It will be out of the scope of this thesis work to explain further different classes of operation. More details can be found in [4].

The simplest configuration of the Doherty architecture is shown in Figure 1.5 which consists of two amplifiers, namely "main" and "peaking" amplifiers. The two amplifiers are connected in a parallel way with a quarter wave transmission line. The quarter wave transmission line is used for impedance transformation.
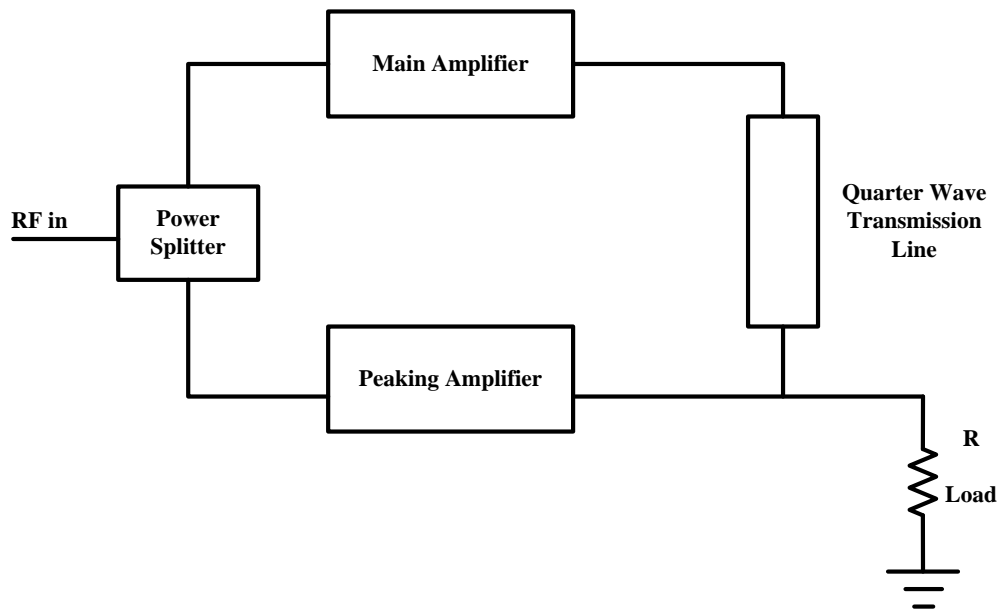
Figure 1.5 Doherty power amplifier architecture

The main amplifier is biased in class AB and the peak amplifier is biased in class C. The role of the quarter wavelength transformer or phase compensation network is to allow the in phase sum on the load of the signals coming from the two active device. The splitter is required at the device gates to properly divide the input signal between the main amplifier and the peak amplifier.

The Doherty PA operating principle is based on the active load pull concept. This concept is based on the principle of applying current from the second source with

coherent phase which have the ability to vary the reactance or resistance of the load. Such

analysis have been presented in [5]. The Active load pull schematic has been depicted in

Figure 1.6.
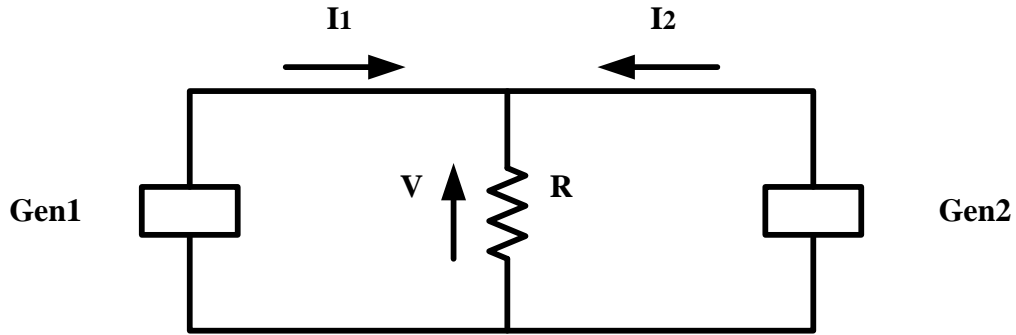
Figure 1.6 Active load modulation schematic

When generator 2 supplies zero current, generator 1 sees a load resistance of R. When

generator 2 starts to supply as well as generator 1, the voltage across the load resistance R

can be calculated as

$$V_L = R[I_1 + I_2] \qquad (16)$$

The resistance seen by generator 1 will be as follows

$$R_1 = R\left[\frac{I_1 + I_2}{I_1}\right] \qquad (17)$$

Similarly, the resistance seen by generator 2 will be as follows

$$R_2 = R\left[\frac{I_1 + I_2}{I_2}\right] \qquad (18)$$

The concept of the load modulation technique can be implemented with transistors if the generators are replaced by the output transconductance of the RF transistors. Therefore, when two transistors are connected in parallel, the impedance seen by each transistor can be modified using a proper biasing. The Doherty configuration results from the combination of two devices with different biasing.

Before discussing the working principle of Doherty power amplifier, it is necessary to analyze the quarter wave transmission line characteristic impedance, Z_{TL}, with respect to the load impedance, Z_{load}. This is explained in appendix.

It is easier to understand the operation of Doherty power amplifier in two stages. The first stage is when the input power is not sufficient to trigger the peak amplifier to contribute to the output power supply. Thus in this stage the total output power is supplied by the carrier amplifier. In this stage, the impedance of the peak amplifier is near to infinity and the load is supplied from the main amplifier.

The second stage is when the input power is sufficient to turn on the peaking amplifier and allow it to become saturated. Thus in this stage the load is provided with maximum power evenly delivered in parallel scenario by main and peaking amplifiers.

The well-known advantages of Doherty power amplifiers are high efficiency and simplicity.

High Efficiency: - The Doherty structure is based on the load pull technique using a quarter wavelength transmission line. This leads to high power added efficiency (PAE) in the 6 dB back off range of the output power.

Simplicity: - The load pull technique that is utilized in the Doherty amplifier is simple and does not involve any complex envelope control circuits.

1.5   Problem Description

One of the major limitations of behavioral models so far is that their parameters are valid for a specific set of operating conditions defined mainly by the signal's average power, its bandwidth, and to a lesser extent its statistics. This means that to maintain the accuracy and performance of a model, its parameters and/or coefficients need to be updated whenever the input signal characteristics change. The updating time increases as the number of coefficients of the model increases and the accuracy of the model is affected when lower model size is selected. Thus, an optimum way of selecting a model size becomes very important to address the need of lower model size without affecting the accuracy of the model. It is important to note here that as the number of coefficients in a model increases beyond a certain size, the additional improvement in the NMSE gets relatively limited. This minor NMSE enhancement is achieved at the expense of higher computation complexity in the model coefficients identification step.

Moreover, as the model size or the total number of coefficients increases, the number of coefficients to be updated following changes of input signal characteristics will increase as well. This will require a huge amount of processing and it adds up to the complexity of the system during the linearization of power amplifiers. It can be seen from the 3rd Generation Partnership Project (3GPP) standard, the change of the signal characteristics eminent due to signal strength, quality and coverage requirements. This thesis addresses

the problem of model complexity arising due to the changes in the signal characteristics (i.e bandwidth of the signal). Part of a model is identified once and remains the same even if signal bandwidth characteristics change occurs. Such type of modeling is named as the bandwidth scalable modeling. This proposed modeling helps to alleviate the problem of high complexity by reducing the complexity of the system during cases where the signal bandwidth changes while keeping the accuracy of the model intact.

1.6   Contribution

This thesis in general contributes in the reduction of total number of model coefficients in areas of power amplifier characterization when it is driven by signals with wider bandwidth. The wider signals used are expected to trigger the memory effects of the power amplifier. The two main contribution of the thesis are mentioned below.

1. A bandwidth scalable behavioral model structure is proposed which result in a significant reduction in regard to the total number of model coefficients that needs to be updated as compared to conventional models. This proposed model alleviates the complexity of the model that may rise during signal characteristic variation due to frequent bandwidth change in the next generation wireless standards such advanced long term evolution and WiMAX.

2. A technique useful for model size selection is another contribution of the thesis. It is on the selection of model dimension for memory polynomial models using a metric that comprises both the complexity and accuracy which is named as complexity aware metric. The proposed complexity aware metric will make the

choice of a better optimum model size that considers two properties, i.e the complexity and the normalized mean square error.

In broader sense this thesis work will contribute to the green wireless communication research area by reducing the amount of power dissipation of base stations front ends due to the reduction of complexity while keeping the performance of the system intact.

1.7   Thesis Organization

The thesis is comprised of five chapters. The first chapter that has been presented so far gives introduction about the basics of communication system, signals in communication systems and nonlinearity in power RF power amplifiers along with the memory effects that have become more significant as part of the distortion introduced by power amplifiers when wide band signals. Further a special type of power amplifier architecture, named as Doherty, is discussed because the measurement in this thesis mainly based on this amplifier since it becomes a widely used type of architecture in emerging wireless transmitters for its power efficiency and other advantages.

In Chapter two, different models that have a suitable property to capture the memory of the system are discussed. The discussion starts from the Volterra series model and its simplified versions like the Wiener and Hammerstein models. Then, different combinations of these two models will be discussed either in a concatenated, parallel or

augmented arrangement. Furthermore, the twin nonlinear two-box model which comprises of a lookup table and a memory polynomial model is discussed. Then models such as dynamic deviation reduction model, generalized memory polynomial and Parallel Lookup table, Memory polynomial and Envelope memory polynomial (PLUME) model are presented. In addition, a new unconventional emerging modeling technique of Neural Network is briefly discussed. Finally the chapter is concluded by a table that summarizes and compares the pros and cons of different types of models that are mentioned in the chapter.

In Chapter three, the newly proposed metric named as complexity aware NMSE metric is proposed. This chapter is organized by first indicating the limitation of the conventional NMSE metric, then the proposed complexity-aware metric performance is compared with the conventional NMSE metric. The comparisons between the conventional and proposed metrics are done on two types of models. Moreover, the comparison is experimentally validated on two types of amplifiers (i.e LDMOS and GaN) with Doherty architecture.

In Chapter four, a bandwidth scalable behavioral model is proposed and validated. The proposed model is benchmarked against the conventional behavioral models. The signals chosen in driving the Doherty power amplifier have bandwidths of 30MHz and 40MHz which are able to trigger the memory effects of the power amplifier. In chapter five the conclusions are stated.

CHAPTER 2

Behavioral Models of RF Power Amplifiers

Power amplifiers have a major effect on the performance of wireless communication systems, which justifies the large number of studies undertaken to understand their behavioral and then to optimize their performance [3-64]. There are three categories of PA models: physical based, circuit based, and black box based or behavioral modeling. The behavioral models or black box approaches is going to be used in this research.

Power amplifiers behavior can be stated as to be made of two components: static (memoryless) distortions and dynamic (memory effects) distortions. The dynamic distortions typically arise for driving signals with 10MHz and wider bandwidths. Several structures have been reported in the literature to model the nonlinear behavior of power amplifiers when driven by wideband signals [6, 7, 9, 15, 17, 20, 61]. These structures include the memory polynomial (MP) model [32] and its derivatives; Volterra model [8], Wiener and Hammerstein structures [6, 9], twin nonlinear two-box (TNTB) models [7], and three-box models such as models that merge the Hammerstein and Wiener models [9]. Among these models, the memory polynomial model is the most preferred as it achieves a trade-off between performance and complexity. It is worth mentioning that MP function can be used as a standalone model as it is the case in the conventional memory polynomial model, or in conjunction with another sub-model as it is the case in the twin-nonlinear two-box model [7]. Moreover, the performances of different models

have been evaluated based on complexity and performance in the work of F. Ghannouchi et al [6, 62].

In this chapter, the main focus is on the two-box modeling technique that is also known as the feed-forward block oriented [10] or modular [11] approach. The two-box model is mainly constructed from memoryless or static nonlinearities and dynamic subsystems. The flexible arrangement of this kind of block structure may lead to different models. The Volterra model gives us a gain in accuracy in predicting the power amplifiers' behavior but pay a lot in terms of complexity as compared to the simpler modified models such as Wiener [12] , Hammerstein, the combination of Wiener and Hammerstein and the forward twin-nonlinear two-box models. These models will be described further in the following sections.

2.1 Volterra Model

This model is the most general and comprehensive model. Power amplifier modeling using the Volterra series has the ability to capture memory effects and accuracy attributed by its kernels. The nonlinearity with M depth of memory is described by the Volterra series in discrete time waveform as follows:

$$y(n) = \sum_{k=1}^{K} y_k(n) \tag{19}$$

where

$$y_k(n) = \sum_{m_1=0}^{M-1} \cdots \sum_{m_k=0}^{M-1} h_k(m_1, \dots, m_k) \prod_{r=1}^{K} x(n - m_r) \tag{20}$$

where $y(n)$ and $x(n)$ are the output and input waveforms, $h_k(m_1, \dots, m_k)$ are the Volterra kernels, K is the highest number of nonlinearity order of the model, and M is maximum memory depth.

The full Volterra series implementation can lead to ill-conditioned matrices during the stage of coefficients extraction. The general formulation in (20) becomes much more complex when the inverse operation is applied for the implementation of the digital predistortion application [13-17]. Moreover, high numbers of coefficients are needed to fully implement the Volterra series. There are more relevant approaches that are applicable for the practical problems of behavioral modeling by variation of memory polynomials. Some of them are described in the following sections.

2.2 Dynamic Deviation Reduction Model

The dynamic deviation reduction (DDR) model [8, 18, 19] adds extra freedom to truncate the Volterra series since it organizes the cross-terms as function of dynamics number.

$$y_{DDR}(n) = y_s(n) + y_d(n)$$

where $y_s(n)$ represents the static characteristic of the system that can be expressed as a power series and $y_d(n)$ is a purely dynamic multi-dimensional convolution with respect to the dynamic deviation.

$$y_{DDR}(n) = \sum_{k=1}^{K} h_k(n)x^k(n) +$$

$$\sum_{k=1}^{K}\left\{\sum_{r=1}^{K}\left[x^{k-r}(n)\sum_{m_1=1}^{M-1} \dots \sum_{m_r=m_{r-1}}^{M-1} h_{k,r}(m_1, \dots, m_r)\prod_{j=1}^{r} x(n-m_j)\right]\right\} \quad (21)$$

where N is the maximum nonlinearity order of the model, M is the memory depth, $h_{k,r}$ are Volterra kernel of the rth deviation order.

The nonlinear dynamics tend to fade with increasing number of orders in several power amplifiers. Thus, higher orders of dynamics are removed from the DDR models. This model has an advantage similar with that of the modified Volterra series models. In DDR, a separation of static nonlinearity and different order of dynamics is possible. This will play a significant role in driving an effective PA linearization approach.

2.3   Generalized Memory Polynomial Model

The generalized memory polynomial (GMP) model is an extension of the MP model with leading and lagging cross-terms [14]. The GMP is formulated as follows:

$$
\begin{aligned}
y_{GMP}(n) =\ & \sum_{m=0}^{M_a} \sum_{k=1}^{K_a} a_{mk} x(n-m)|x(n-m)|^{k-1} \\
& + \sum_{m=0}^{M_b} \sum_{k=1}^{K_b} \sum_{l=1}^{L_b} b_{mkl} x(n-m)|x(n-m-l)|^{k-1} \\
& + \sum_{m=1}^{M_c} \sum_{k=2}^{K_c} \sum_{l=1}^{L_c} c_{mkl} x(n-m)|x(n-m+l)|^{k-1}
\end{aligned}
$$

(22)

where the $x(n)$ and $y_{GMP}(n)$ are the input and the generalized memory polynomial estimated output, respectively. K_a, K_b and K_c are the nonlinearity orders for the envelope terms, the lagging envelope terms and the leading envelope terms, respectively. M_a, M_b and M_c are the memory depth for the signal and envelope terms, the signal and lagging

22

envelope terms and for the signal and leading envelope terms, respectively. L_b and L_c are the lagging and leading cross-terms indexes, respectively. a_{mk} b_{mkl} and c_{mkl} are the coefficients of the signal and envelope terms, coefficients of the signal and lagging envelope terms, and coefficient of the signal and leading terms, respectively.

The GMP model, similarly with some of the reduced forms of the Volterra model, has an advantage on the linearity of the coefficients as it can be stated in equation (22). This model considers both the lagging and leading cross-terms unlike the MP models because the GMP introduces cross-terms. Thus, the advantage of the GMP model is that its ability to include the cross-term coefficients and keep the linearity of the coefficients which plays significant role in the stability and computational complexity of the algorithm.

2.4   Memory Polynomial /Envelope MP Models

The memory polynomial model is formulated from the Volterra series model pruned to keep only the diagonal terms and no cross-terms. The formulation of the model that is presented in [20] is selected. Thus, the equation of the memory polynomial model can be formulated as

$$y_{MP}(n) = \sum_{m=0}^{M} \sum_{k=1}^{K} a_{km} x(n-m)|x(n-m)|^{k-1} \qquad (23)$$

where $x(n)$ and $y_{MP}(n)$ are the baseband complex input and output, respectively. a_{km} are the polynomial coefficient, K is the polynomial function order and M is the memory depth.

On a similar discussion, when the combination of $x(n)|x(n-m)|^{k-1}$ is selected from pruned Volterra series, a new model named envelope memory polynomial (EMP) is obtained. The EMP can be formulated as follows

$$y_{EMP}(n) = \sum_{m=0}^{M}\sum_{k=1}^{K} a_{km}x(n)|x(n-m)|^{k-1} \tag{24}$$

where $x(n)$ and $y_{EMP}(n)$ are the baseband complex input and output, respectively. a_{km} are the polynomial coefficient, K is the polynomial function order and M is the memory depth

The EMP model is proven to be effective in predistortion applications [14, 21-31] of power amplifiers. Besides a low complexity behavioral models that are suitable for power amplifiers with memory effects have been presented in [32] and [33]. Moreover a compact EMP model that is suitable for weakly nonlinear power amplifiers is discussed in [29]. A Compact EMP model function is presented as follows

$$y_{Compact\ EMP}(n) = \sum_{m=0}^{M}\sum_{K=1}^{K} a_{km}|x(n-m)|^{k-1} \tag{25}$$

where $x(\text{n})$ and $y_{Compact\ EMP}(\text{n})$ are the baseband complex input and output, respectively. a_{km} are the polynomial coefficient, K is the polynomial function order and M is the memory depth

The compact EMP takes the advantage of the dependency of power amplifier nonlinearity on the magnitude of the input signal. Unlike the EMP model, the compact EMP can be implemented in radio frequency and baseband digital predistorters with comparable performance with EMP.

2.5   Memoryless Polynomial Model

The memoryless polynomial unlike the memory polynomial model can be formulated as

$$y_{Memoryless\ Polynomial}(n) = \sum_{k=1}^{K} a_k x^k(n) \tag{26}$$

where $x(n)$ is the input signal and a_k is the kth nonlinear coefficient.

The memoryless polynomial model is commonly implemented as look-up table (LUT). This is a relatively simple model where a wide range of possible amplifier inputs and their corresponding (complex) outputs are saved in a table so that for any given input, the appropriate output is found by interpolating the table entries. The LUT is given by:

$$y_{lut}(n) = G(|x(n)|) \cdot x(n) \tag{27}$$

where $x(n)$ is the input signal and $G(|x(n)|)$ is the instantaneous complex gain of the PA.

This model is widely used in modeling and predistortion of power amplifiers. The AM/AM and AM/PM characteristics of a power amplifier are used to construct tables. In [34] , multiple LUTs for different power levels are used in case of power level changes of the driving signals which show a faster response to such change in PA characteristics. The LUT is often used to implement a memoryless polynomial. However, it can be built by averaging the measured characteristics of the PA.

2.6　Wiener Model

One of the modified cases of the Volterra series approach is the Wiener model. It consists of a linear filter (h) followed by a memoryless nonlinearity as shown in Figure 2.1. It has been studied as a general means for nonlinear system identification in [35, 36] and for predistortion application in transmitters [37, 38]

$x(n)$ → [h] → [NL] → $y(n)$
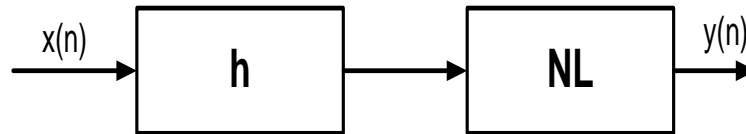
Figure 2.1 Block diagram of the Wiener model

The Wiener model can be formulated as follows:

$$y(n) = \sum_{k=1}^{K} a_k \left[\sum_{m=0}^{M} h(m)x(n-m) \right]^k \tag{28}$$

where K is the maximum nonlinearity order, M is the memory depth, a_k are the nonlinearity polynomial coefficients of the Wiener model, $x(n)$ and $y(n)$ are the input and output of the model, respectively.

The Wiener model combines memory effects and nonlinearity in a simple way. However the accuracy of this model is very limited for most power amplifiers. Besides, the output of equation (28) depends on the coefficients of $h(m)$ nonlinearly. This makes the estimation of $h(m)$ coefficients more difficult than that of Hammerstein models which is described in the next section.

26

2.7 Hammerstein Model

The Hammerstein model is one of the simplified models of Volterra series with memory nonlinearity [36]. It is formed by using the nonlinearity function (NL) and the linear system (g) in such a way that the first is followed by the second as shown in the Figure 2.2.
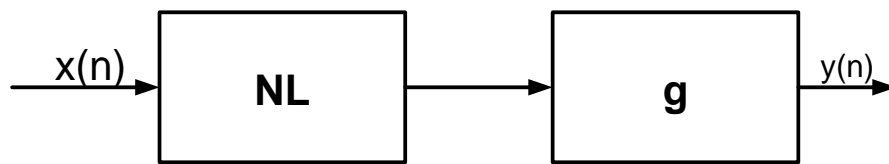
Figure 2.2 Block Diagram of the Hammerstein model

The Hammerstein model can be formulated as,

$$y(n) = \sum_{m=0}^{M} g(m)[a_k \sum_{k=1}^{K} x^k(n-m)] \tag{29}$$

This memory nonlinear formulation has a property of being linear in the parameters $g(m)a_k$. However the formulation has a limitation in effectiveness of the predistortion. It has been commented in [14] that the Hammerstein and Wiener models form mutual inverses if their nonlinear polynomials are one to one inverses and the linear filters in both types of models have stable inverses.

2.8 Wiener-Hammerstein Model

The Wiener and Hammerstein models [63] can be combined by cascading the linear filter followed by a memoryless nonlinearity, and another linear filter.
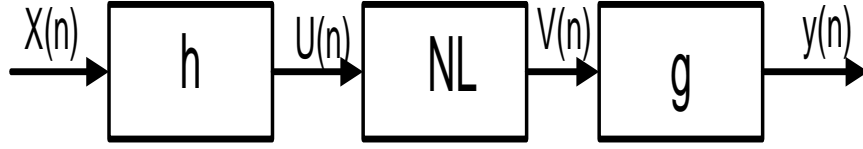
Figure 2.3 Block diagram of the Wiener-Hammerstein model

The formulation of the Wiener-Hammerstein model is as follows

$$u(n) = \sum_{m_1=0}^{M} h(m_1)x(n - m_1) \tag{30}$$

$$v(n) = \sum_{k=1}^{K} a_k [u(n)]^k = \sum_{k=1}^{K} a_k \left[\sum_{m_1=0}^{M} h(m_1)x(n - m_1) \right]^k \tag{31}$$

where the $u(n)$ and $v(n)$ are the intermediate variables; a_k are the memoryles nonlinear coefficients of the second box; M and $h(m_1)$ are the number of taps (memory depth) and the impulse response of the first filter which is located in the upstream of the nonlinear memoryless box, respectively.

Therefore, the output of the Wiener-Hammerstein model is represented as follows:

$$y(n) = \sum_{m_2=0}^{M} g(m_2) \; v(n - m_2) \tag{32}$$

Accordingly,

$$y(n) = \sum_{m_2=0}^{M_2} g(m_2) \sum_{k=1}^{K} a_k \left[\sum_{m_1=0}^{M_1} h(m_1)x(n - m_1 - m_2) \right]^k \tag{33}$$

The estimation of the parameters in each block of the wiener-Hammerstein is not simple because the model output is not linear with respect to its parameters.

28

2.9 Hammerstein-Wiener Model

The Hammerstein-Wiener model is also a combination of the Hammerstein and Wiener Models such that a linear time invariant filter is preceded and followed by static nonlinearity [39].
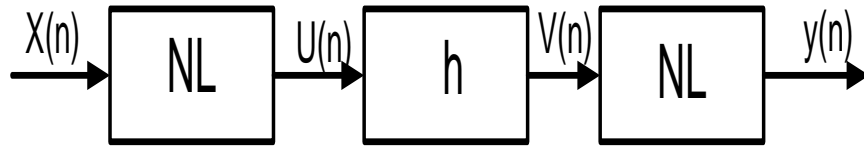
Figure 2.4 Block diagram of the Hammerstein-Wiener model

The first box of the nonlinearity function can be represented as

$$u(n) = \sum_{k_1=1}^{K} a_{k_1} [x(n)]^{k_1} \tag{34}$$

Then, the output $u(n)$ from the first box will be the input of the linear filter h, which can be formulated as such

$$v(n) = \sum_{m=0}^{M} h(m)u(n-m) = \sum_{m=0}^{M} h(m) \left[\sum_{k_1=1}^{K} a_{k_1} [x(n-m)]^{k_1} \right] \tag{35}$$

The output of the linear filter h will be applied at the input of the second nonlinear box, which can be stated as follows.

$$y(n) = \sum_{k_2=1}^{K} a_{k_2} [v(n)]^{k_2} \tag{36}$$

Finally the Hammerstein-Wiener model can be stated as

$$y(n) = \sum_{k_2=1}^{K} a_{k_2} \left[\sum_{m=0}^{M} h(m) \left[\sum_{k_1=1}^{K} a_{k_1} [x(n-m)]^{k_1} \right] \right]^{k_2} \tag{37}$$

Where $x(n)$ and $y(n)$ are the input and output signals of the Hammerstein-Wiener model, respectively. $u(n)$ and $v(n)$ represent intermediate signals that are not directly accessible.

The concatenated models formulation, either Hammerstein-Wiener or Wiener-Hammerstein, are more complex compared to Wiener and Hammerstein models. However the three-box cascaded models provide more generality.

2.10 Dual-branch Wiener-Hammerstein Model

The dual-branch Wiener-Hammerstein model [61] is made up of two branches that are connected in parallel. One of the parallel branches is a Wiener model and the other is Hammerstein model. The model structure is illustrated in the Figure 2.5.
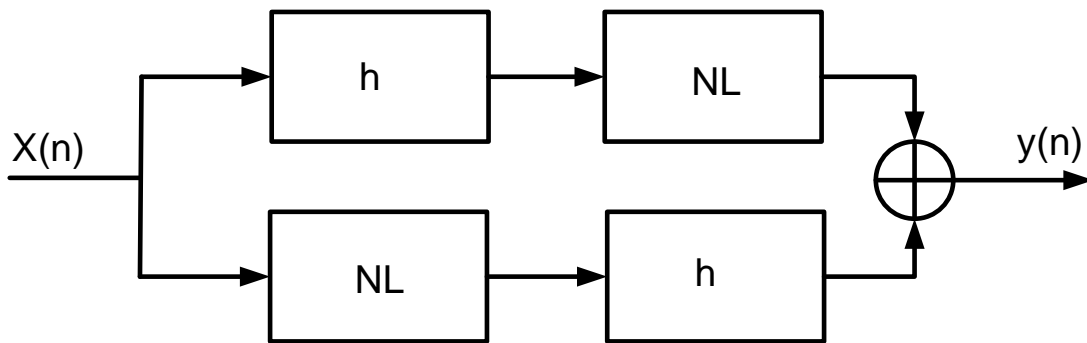
Figure 2.5 Block diagram of the dual-branch Wiener-Hammerstein model

The dual-branch Wiener-Hammerstein model can be formulated by the summation of the output of each of the branches which will have a similar formulation as described in equations of (28) and (29)

$$y_{Dual-branch\,W-H}(n) = y_{Hammerstein}(n) + y_{Wiener}(n) \tag{38}$$

The expected advantage of this model is the nonlinear behaviors of the power amplifiers to be captured by either one of the model branches or both.

2.11   Augmented Wiener Model

The augmented Wiener model [41] is an extension of the Wiener model. It consists of a parallel second branch of nonlinearity with the FIR filter box of the Wiener model and the nonlinearity box of the wiener model is represented by a memoryless nonlinear functions commonly implemented or referred to LUT. The structure of this model is shown in Figure 2.6.
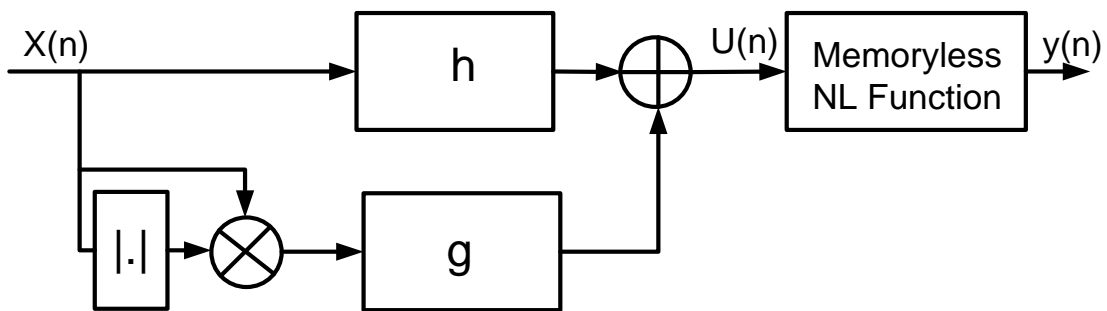
Figure 2.6 Block diagram of the augmented Wiener model

According to the structure the augmented Wiener model has the following formulation

$$U(n) = \sum_{m_1=0}^{M_1} h_{m_1} x(n - m_1) + \sum_{m_2=0}^{M_2} g_{m_2} x(n)|x(n - m_2)| \qquad (39)$$

where h_{m_1} and g_{m_2} are the coefficients of the first and second filters indicated in Figure 2.6 as h and g, respectively. M_1 and M_2 are the memory depth of the first and second filter, respectively.

The model's output is

$$y_{Augmented\ Wiener}(n) = \sum_{k=1}^{K} a_k U^k(n) \qquad (40)$$

where $x(n)$ is the input signal , a_k is the kth nonlinear coefficient and $U(n)$ is the intermediate signal generated within the model as it is stated in equation (39).

2.12 Augmented Hammerstein Model

The augmented Hammerstein model [42] consists of memoryless nonlinear function and two filters connected in parallel as shown in the Figure 2.7.
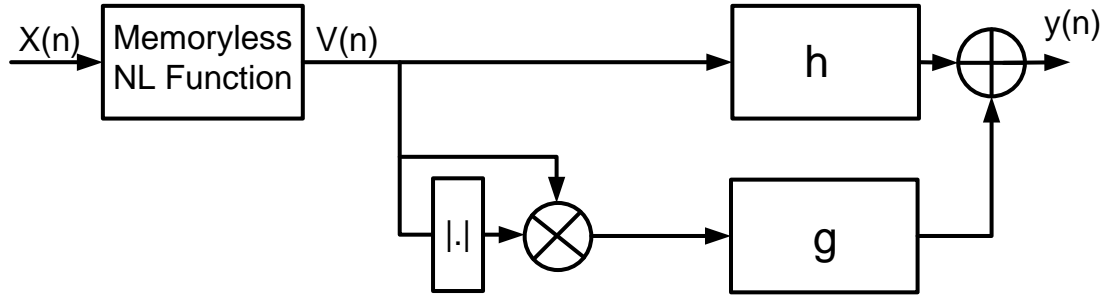
Figure 2.7 Block diagram of the augmented Hammerstein model

In the augmented Hammerstein model, the memoryless nonlinear function is located as the first block. The output of memoryless nonlinear function is represented as $V(n)$.

$$V(n) = \sum_{k=1}^{K} a_k x^k(n) \tag{41}$$

where $x(n)$ is the input signal , a_k is the kth nonlinear coefficient and $U(n)$ is the intermediate signal generated within the model.

$$y(n) = \sum_{m_1=0}^{M_1} h_{m_1} V(n - m_1) + \sum_{m_2=0}^{M_2} g_{m_2} V(n)|V(n - m_2| \tag{42}$$

The augmented Wiener and augmented Hammerstein models have an advantage by adding the second filter branch. It gives the augmented model more degrees of freedom in characterizing nonlinearity and memory effects of the power amplifier.

2.13 Twin-Nonlinear Two-Box (TNTB) Model

The Twin-Nonlinear Two-Box (TNTB) models [7] represent a family of models suitable for power amplifiers with memory effects. These models are obtained by combining

components taken from the following two classes: memoryless (or static) and dynamic systems. The dynamic part can be implemented as a low order memory polynomial while the memoryless nonlinearity can be implemented by a lookup table.

$x(n)$ → **Look-up Table** → **Memory Polynomial** → $y(n)$

(a)

$x(n)$ → **Memory Polynomial** → **Look-up Table** → $y(n)$

(b)

$x(n)$ → **Memory Polynomial**, **Look-up Table** → ⊕ → $y(n)$
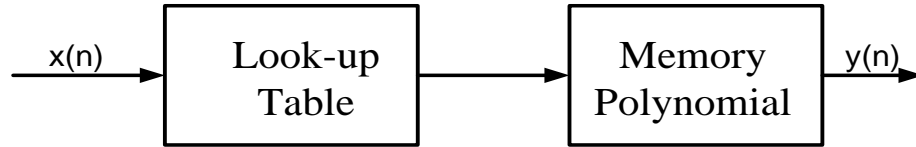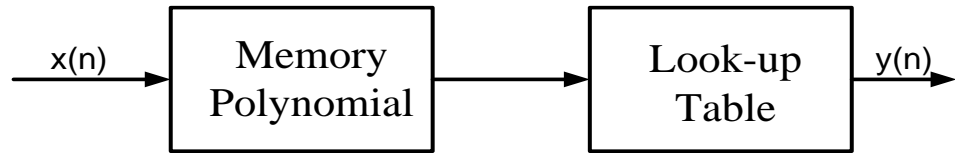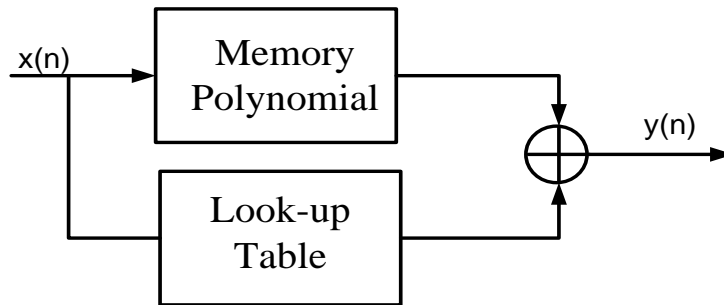
(c)

Figure 2.8 Block diagram of the twin-nonlinear two-box models a) forward b) reverse c) parallel

Each different TNTB model consists of a cascaded Look-up table and memory polynomial models. In the forward TNTB (FTNTB) model, the memory polynomial is placed in the downstream of the look-up table. In the reverse TNTB (RTNTB) model, the memory polynomial is placed in the upstream of the look-up table. The memory

34

polynomial and look-up table are placed in parallel in parallel TNTB (PTNTB) model. The functions and formulas of the memory polynomial and look-up table remain the same in all three types of TNTB models as they are described in sections 2.4 and 2.5, respectively.

The identification process in twin-nonlinear two-box modes is composed of two steps. The process of extraction of the highly nonlinear memoryless behavior of the power amplifier comes first. This memoryless behavior is represented by the look-up table box. The second step of identification uses the intermediate output of the look-up table as input to the memory polynomial model in case of FTNTB model while the intermediate input of the look-up table considered as the output of the memory polynomial in case of RTNTB model. In case of the PTNTB, the output of the memory polynomial will be deduced by subtracting the lookup table output from the measured output signal. Then parameters of the memory polynomial box will be identified then after in all the three types of TNTB models.

When the TNTB model's parameter identification is compared to that of the MP, it requires one additional step than that of MP. However, this increase in complexity is compensated by the low number of parameters to be used in the model.

2.14 PLUME Model

The "PLUME" model refers to the parallel connection of a look-up table, memory polynomial and envelop memory polynomial [43]. This model can be considered as an

extension of the parallel twin-nonlinear two-box model since an additional box of envelope memory polynomial is added to it.
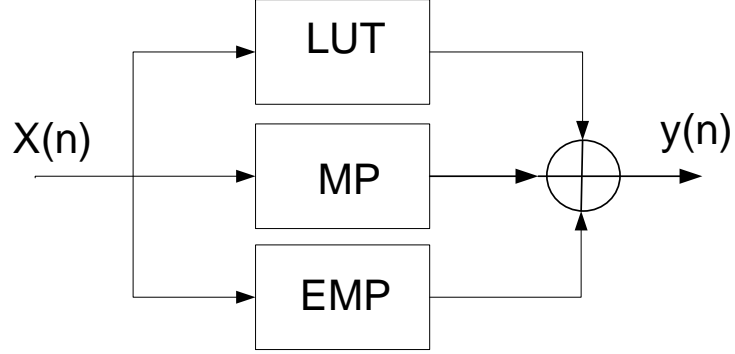
Figure 2.9 Block diagram of the PLUME three-box model

The first box, which is represented as LUT, is a memoryless nonlinear function that was described in (26). The second box, which is represented as MP, is a low order memory polynomial function. The third box, which is indicated as EMP, is the envelop memory polynomial model.

$$y(n) = y_{LUT}(n) + y_{MP}(n) + y_{EMP}(n) \tag{43}$$

where y_{LUT} , $y_{MP}(n)$ and y_{EMP} are LUT model estimated output, the MP model estimated output and the EMP model estimated output, respectively. The formulation of each box is given as:

$$y_{LUT}(n) = G(|x(n)|) \cdot x(n)$$

$$y_{MP}(n) = \sum_{k=1}^{N_{MP}} \sum_{m=0}^{M_{MP}} a_{km} x(n-m)|x(n-m)|^{k-1}$$

36

$$y_{EMP}(n) = \sum_{k=1}^{N_{EMP}} \sum_{m=0}^{M_{EMP}} b_{km} x(n) |x(n-m)|^{k-1}$$

(44)

where (n) , G , a_{km} and b_{km} are the input signal, the instantaneous gain of the LUT model, the coefficients of the MP model and the coefficients of the EMP model respectively. N_{MP} and M_{MP} are the nonlinearity and memory depth of the MP sub-model, respectively. N_{EMP} and M_{EMP} are the nonlinearity and memory depth of the EMP sub-model, respectively.

The PLUME model further increases the accuracy of the behavioral model when it is compared to that of the parallel twin-nonlinear two-box model because of the additional cross-terms incorporated through the addition of envelope memory polynomial function. While the increase in accuracy is mentioned as an advantage for the PLUME model, the increment of the total number coefficients are perceived as the major disadvantage. However, the increase in the number of coefficients can be controlled by optimum choice of the EMP model dimensions. The PLUME model has lower number of coefficients and gives a similar performance as it is compared to the GMP model.

2.15 Feed-forward Neural Network based Model

Besides models that have been discussed so far, there are also other models that use alternative techniques. These models can be collectively called neural network (NN) based models. The neural network based models use the artificial neural network

information processing techniques that are currently used in wide areas of engineering. These techniques are inspired from the observation and study of the human mind neurology in the sense that how the human mind learn from observation and abstraction.

The feed-forward-NNs act as the bases of many of the NN structures. The basic structure is a single input and single output feed-forward-NN uses complex input and output signal data. Thus, the feed-forward-NN topologies [44] lead to heavy calculation with the introduction of the complex weight and activation output which can be illustrated as follows :

$$y(x(t)) = \sum_{N_l} w_l f_l \{ \sum_{N_{l-1}} w_{l-1} f_{l-1} [\dots \sum_{N_1} x(t)] + b_{l-1} \} + b_l \qquad (45)$$

where $N_l, N_{l-1}, N_{l-2} \dots N_1$ represents the number of neurons in each layers, l is the total number layers. w_l and f_l are the weights and activations function in the lth layer, respectively.

The feed-forward-NN model identification is dependent on a selection of a suitable network topology and the model dimensions which are the number of layers and number of neurons in each layer, and the complex waveforms of phase information.

2.16 Model Comparison Summary

In the following table, a summary of different models is stated in comparison form including their advantages and disadvantages along with the formula of the models for

ease of reference. In all these models $x(n)$ and $y(n)$ refer the model's input and output waveforms, respectively. The parameters of these models were defined in the previous sections.

Table 2.1 Model comparison summary

Models	Formulas	Advantaged	Disadvantage
Volterra	$$y(n) = \sum_{k=1}^{K} \sum_{m_1=0}^{M} \cdots \sum_{m_p=0}^{M} h_p(m_1, \ldots, m_p) \prod_{l=1}^{k} x(n - m_l)$$	Excellent accuracy and captures nonlinearity and memory effects of a system.	Highest number of coefficients to fully implement the model and ill conditioned matrices during inversion.
DDR	$$y(n) = \sum_{p=1}^{N} h_{p,0} x(n)|x(n)|^{p-1}$$ $$+ \sum_{p=1}^{N} \sum_{m_1=1}^{M} h_{p,m_1} x(n - m_1)|x(n)|^{p-1}$$ $$+ \sum_{p=1}^{N} \sum_{m_2=1}^{M} h_{p,m_2} x(n - m_2) x^2(n)|x(n)|^{p-3}$$	Separation of static nonlinearity and different order dynamics after model extraction. The model has better accuracy compared to memory polynomial model.	More coefficients when it is compared with MP and GMP but less coefficients when compared with Volterra model.

Models	Formulas	Advantaged	Disadvantage
GMP	$y(n) = \sum_{m=0}^{M_a}\sum_{k=1}^{K_a} a_{mk}x(n-m)\|x(n-m)\|^{k-1}$ $+ \sum_{m=0}^{M_b}\sum_{k=1}^{K_b}\sum_{l=1}^{L_b} b_{mkl}x(n-m)\|x(n-m-l)\|^{k-1}$ $+ \sum_{m=1}^{M_c}\sum_{k=2}^{K_c}\sum_{l=1}^{L_c} c_{mkl}x(n-m)\|x(n-m+l)\|^{k-1}$	Cross-terms are included in such a way that the coefficients are related in a linear formulation. Thus, simple and robust estimation is possible.	Increased number of coefficients, time consuming as compared to MP or EMP and unstable use in DPD application.
Memory Polynomial	$y(n) = \sum_{k=1}^{K}\sum_{m=0}^{M} a_{km}x(n)\|x(n-m)\|^{k-1}$	Simple definition and low complexity nonlinear memory effects can be characterized	Ill-conditioned matrices during inversion.
LUT	$y(n) = G(\|x(n)\|) \cdot x(n)$	Easy for pre-distortion application and memoryless modeling.	Cannot capture behavior of system with memory.
Wiener	$y(n) = \sum_{k=1}^{K} a_k \left[\sum_{m=0}^{M} h(m)x(n-m)\right]^k$	Separation of the nonlinear and memory in simple way and ability to capture linear memory effects.	Output waveform is nonlinearly related to the parameter to be estimated.
Hammerstein	$y(n) = \sum_{m=0}^{M} g(m)\left[a_k \sum_{k=1}^{K} x^k(n-m)\right]$	Separation of the nonlinearity and memory of a system and ease of identification.	Includes only linear memory effects.

Models	Formulas	Advantaged	Disadvantage
Wiener-Hammerstein	$$y(n) = \sum_{m_2=0}^{M_2} g(m_2) \sum_{k=1}^{K} a_k \left[\sum_{m_1=0}^{M_1} h(m_1)x(n-m_1-m_2) \right]^k$$	Tractable and reliable since it has an ability to capture more information of the system.	Complex and the output waveform is nonlinearly related to the parameter to be estimated.
Hammerstein-Wiener	$$y(n) = \sum_{k_2=1}^{K} a_{k_2} \left[\sum_{m=0}^{M} h(m) \left[\sum_{k_1=1}^{K} a_{k_1}[x(n-m)]^{k_1} \right] \right]^{k_2}$$	Tractable and reliable since it has an ability to capture more information of the system	Complex and increase in total number of coefficients.
Dual-branch Hammerstein-Wiener	$$y(n) = \sum_{m=0}^{M} g(m) \left[a_k \sum_{k=1}^{K} x^k(n-m) \right]$$ $$+ \sum_{k=1}^{K} a_k \left[\sum_{m=0}^{M} h(m)x(n-m) \right]^k$$	Combines the advantages of both the Wiener and Hammerstein models.	Increase of model complexity along with problems of Wiener model coefficients nonlinearity.
Augmented Wiener	$$U(n) = \sum_{m_1=0}^{M_1} h_{m_1}x(n-m_1) + \sum_{m_2=0}^{M_2} g_{m_2}x(n)|x(n-m_2)|$$ $$y_{Aug\ Wiener}(n) = G(|U(n)|)U(n)$$	Ability to include nonlinear memory effects.	Additional complexity when it is compared to Wiener model.
Augmented Hammerstein	$$y(n) = \sum_{m_1=0}^{M_1} h_{m_1}V(n-m_1)$$ $$+ \sum_{m_2=0}^{M_2} g_{m_2}V(n)|V(n-m_2)|$$ $$Where\ V(n) = G(|x(n)|)x(n)$$	Ability to include nonlinear memory effects.	Additional Complexity when it is compared with Hammerstein model
FTNTB	$$y(n) = \sum_{k=1}^{K} \sum_{m=0}^{M} a_{km}(G(|x(n-m)|) \cdot x(n-m))^k)$$	Separation of the static and memory effects.	No cross-terms are included in the MP box.

Models	Formulas	Advantaged	Disadvantage
RTNTB	$$U(n) = \sum_{k=1}^{K} \sum_{m=0}^{M} a_{km} x(n)|x(n-m)|^{k-1}$$ $$y(n) = G(|U(n)|)U(n)$$	Separation of the static and memory effects.	No cross-terms are included in the MP box. Slightly higher complexity and lower performance than that of FTNTB and PTNTB
PTNTB	$$y(n) = G(|x(n)|) \cdot x(n) + \sum_{k=1}^{K} \sum_{m=0}^{M} a_{km} x(n)|x(n-m)|^{k-1}$$	Separation of the static and memory effects. Slightly lower complexity and higher performance than that of FTNTB and PTNTB	No cross-terms are included in the MP box.
PLUME	$$y(n) = \sum_{k=1}^{K_{MP}} \sum_{m=0}^{M_{MP}} a_{km} x(n-m)|x(n-m)|^{k-1}$$ $$+ \sum_{k=1}^{K_{EMP}} \sum_{m=0}^{M_{EMP}} b_{km} x(n)|x(n-m)|^{k-1}$$ $$+ \quad G(|x_{lut-in}(n)|) \cdot x_{lut-in}(n)$$	Further enhancement on accuracy due to the addition of EMP as compared to TNTB models	Increase in total number of coefficients but still lower than GMP

In conclusion, this chapter discussed several power amplifier behavioral models. It can be noticed that as one move from the simple classical models to the more complex and advanced models of the memory polynomial, the accuracy and effectiveness of the model generally increase. However, the computational complexity is found to increase along with the increase of the accuracy of the developed models. In this thesis two-box models have been chosen among the different models discussed in this chapter for the

implementation of the bandwidth scalable behavioral models. The rationale behind this

choice is detailed in chapter 4.

CHAPTER 3

COMPLEXITY-AWARE-NMSE "CAN" METRIC FOR DIMENTION ESTIMATION OF MEMORY POLYNOMIAL BASED POWER AMPLIFIERS BEHAVIORAL MODELS

The memory polynomial model is widely used for the behavioral modeling of radiofrequency nonlinear power amplifiers having memory effects. One challenging task related to this model is the selection of its dimension which is defined by the nonlinearity order and the memory depth. This work presents an approach suitable for the selection of the model dimension in memory polynomial based power amplifiers' behavioral models. The proposed approach uses a hybrid criterion that takes into account the model accuracy and its complexity. The proposed technique was tested on two memory polynomial based behavioral models namely the single-box memory polynomial model and the forward twin-nonlinear two-box model. Experimental validation carried out using experimental data of two Doherty power amplifiers, built using different transistor technologies and tested with two different signals, illustrates consistent advantages of the proposed technique as it significantly reduces the model dimension without compromising its performance.

3.1 Motivation

Among all the models, memory polynomial based models are commonly used since they achieve a reasonable trade-off between accuracy and complexity. However, even though they are popular, memory polynomial based models still have a major aspect that lacks investigation. In fact, the memory polynomial function requires the selection of its dimension (mainly the nonlinearity order and memory depth) and the identification of the corresponding coefficients. However, there is no straightforward systematic approach that allows for the proper selection of the model dimension. This is a critical aspect since over estimating the model dimension will result in additional identification and implementation complexity, and under estimation of the model dimensions will affect the accuracy of the model.

This chapter proposes a complexity-aware normalized mean squared error (labeled "CAN") metric suitable for the model dimension estimation in memory polynomial based models. The proposed metric offers a comprehensive quantification of the model performance as it considers both its accuracy and complexity. The CAN metric can be applied to find out the dimensions of the memory polynomial function in a wide range of models such as the conventional memory polynomial model, the envelope memory polynomial model, the generalized memory polynomial model, and the twin-nonlinear two-box model.

In Section 3.2, the limitations of conventional NMSE metric for the model dimension evaluation are discussed. In Section 3.3, the complexity-aware-NMSE metric is introduced and its performances benchmarked against those of the NMSE metric for the

case of the conventional single-box memory polynomial model. In Section 3.4, the CAN metric is applied to determine the dimensions of the memory polynomial function in the forward twin-nonlinear two-box model.

3.2 Limitation of Conventional NMSE Metric

When driven by signals with wide bandwidths (10MHz or wider), power amplifiers exhibit dynamic nonlinear behavior. The Volterra series represent the most comprehensive model for dynamic nonlinear systems. However, this model results in an unrealistically high number of coefficients as the nonlinearity order and memory depth of the system increase. Conversely, the memory polynomial model which corresponds to the diagonal terms of the Volterra series is considered among the most popular models for dynamic nonlinear systems as it achieves an acceptable tradeoff between the model performance expressed in term of its accuracy and the model's complexity evaluated in terms of its number of coefficients.

It is worth mentioning that the memory polynomial function can be used as a standalone model as it is the case in the conventional memory polynomial model [20], or in conjunction with another sub-model as it is the case in the twin-nonlinear two-box model [7]. The study presented in this chapter will initially focus on the conventional memory polynomial model, and will be extended in Section 3.4 to the case of the forward twin-nonlinear two-box model.

The primary device under test (DUT) used in the experiments is a 300-Watt LDMOS based Doherty power amplifier designed for the 2100MHz frequency band. This DUT was characterized using a 40MHz WCDMA signal using a custom-built characterization platform [49]. First, the measured data was de-embedded to the device under test input and output reference planes by compensating for the attenuation between the measurement planes and the reference planes. Also, time alignment was performed to compensate for the delay between the measured input and output waveforms. The time aligned input and output complex baseband waveforms of the DUT were then used to derive its behavioral model. The measured AM/AM and AM/PM characteristics of the device under test reported in Figure 3.1 show its strong memory effects as it can be noticed through the significant dispersion in the AM/AM and AM/PM characteristics.
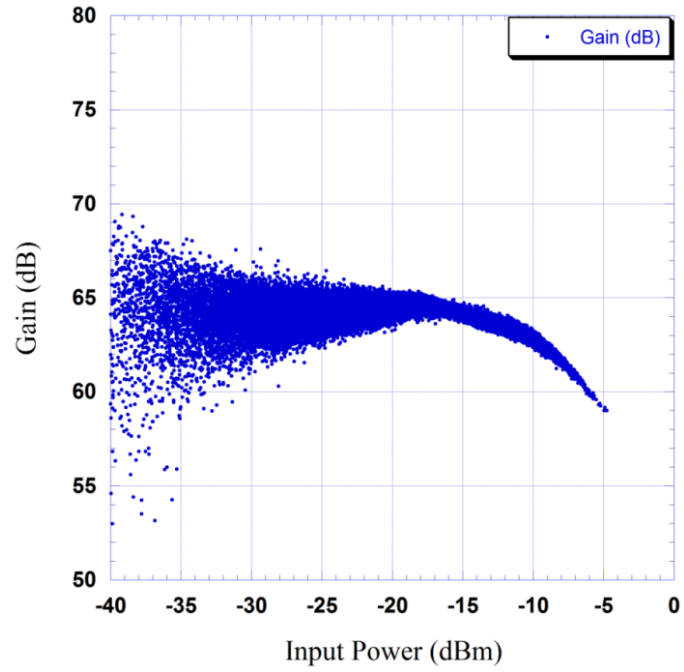
(a)
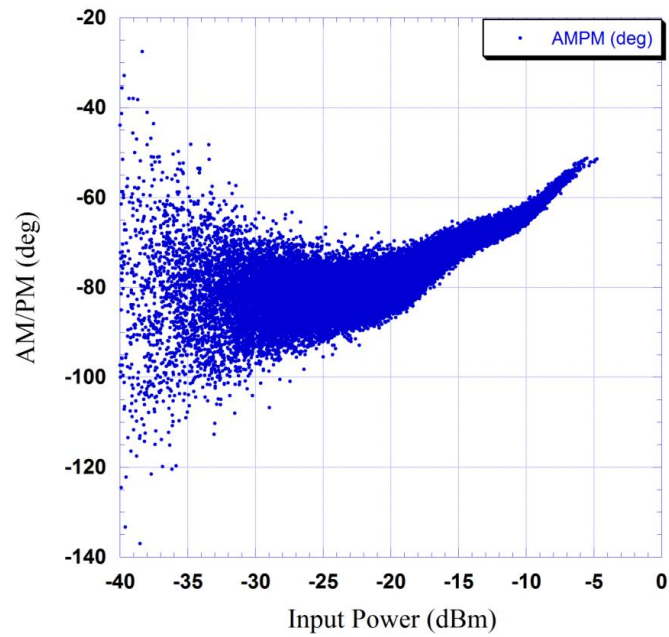
(b)

Figure 3.1 Measured characteristics of the device under test. (a) AM/AM characteristics, (b) AM/PM characteristics.

The measurement data was then processed to identify the memory polynomial based model of the device under test by solving the corresponding linear system as described in [49]. Since the model dimensions are unknown, the nonlinearity order and the number of branches were swept over a wide range. The nonlinearity order was varied from 3 to 12, while the number of branches was successively increased from 1 to 10.

The performance of each of the 100 models identified was evaluated in terms of the normalized mean squared error metric given by:

$$NMSE_{dB} = 10log_{10}\left(\frac{\sum_{n=1}^{L}|y(n)-y_{estim}(n)|^2}{\sum_{n=1}^{L}|y(n)|^2}\right) \tag{46}$$

where $y(n)$ and $y_{estim}(n)$ are the measured and estimated waveforms at the output of the device under test, respectively. L is the number of samples in each of these waveforms.

The 3D plot of the NMSE versus the model parameters (M and N) is reported in Figure 3.2. This figure shows that the NMSE improves as the number of coefficients is increased. Most importantly, the NMSE curve presents an asymptotic behavior for high nonlinearity orders and high number of branches where increasing the model dimension leads to minor improvement in the model accuracy. This can be clearly observed in the plots reported in Figure 3.3 in which the NMSE is plotted as a function of the number of branches for various nonlinearity orders. According to this figure, increasing the nonlinearity order beyond 9 does not improve the model performance. However, as the

number of branches increases, the model's accuracy is improved. Thus, the minimum NMSE is obtained for a model with N=9 and M=10. This model has 90 coefficients and achieves an NMSE of -35.9dB.
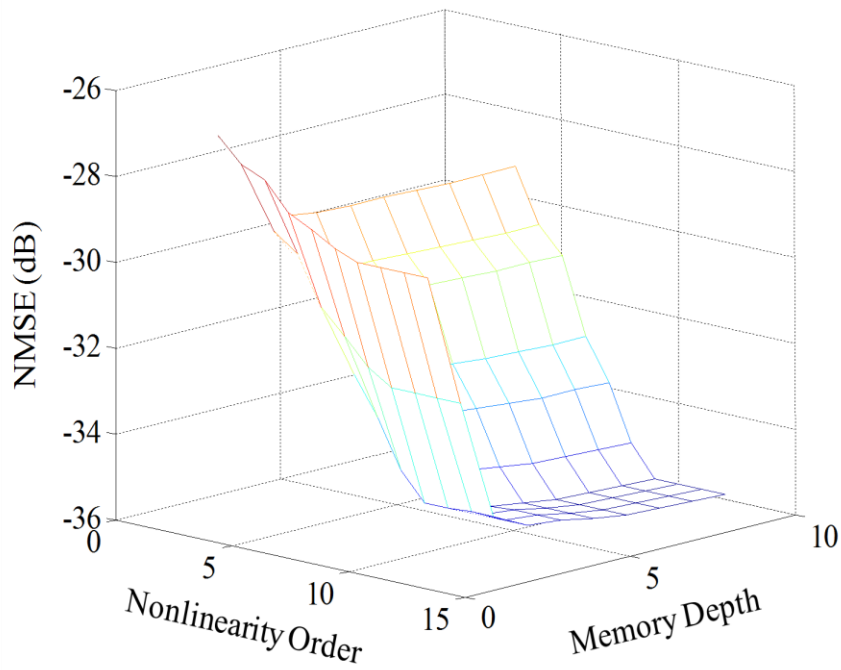
Figure 3.2 Calculated NMSE versus the model's parameters

It is important to note here that as the number of branches increases, the additional improvement in the NMSE gets relatively limited. However, this minor NMSE enhancement is achieved at the expense of higher computation complexity in the model's coefficients identification step. Thus, there is a need for an objective metric that will allow for the automated selection of the appropriate model dimensions.
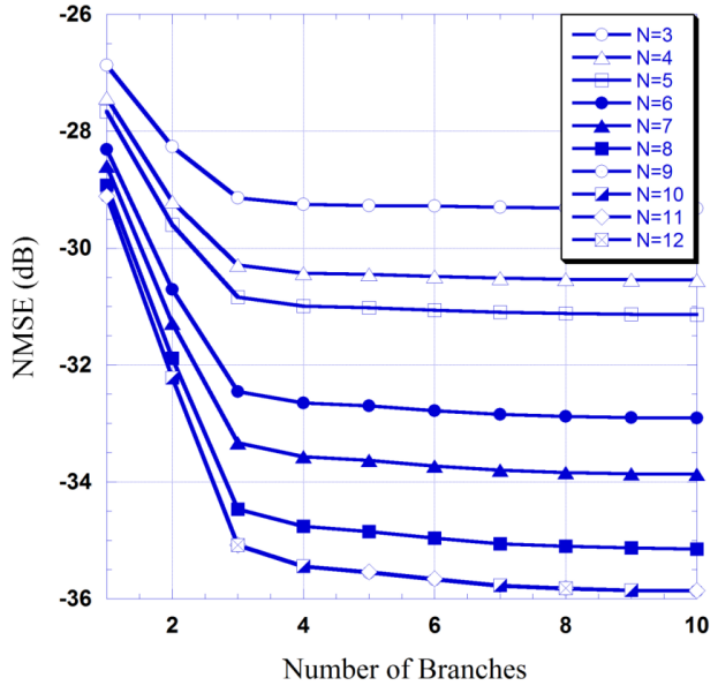
Figure 3.3 Calculated NMSE of the memory polynomial model as a function of the model's number of branches for different nonlinearity orders.

.

3.3 Proposed Complexity-Aware-NMSE Metric

As illustrated through the results reported in Figure 3.3, the NMSE of the memory polynomial model improves as the model's number of coefficients increases. However, this NMSE enhancement stagnates gradually. For example, for the considered set of measurements, the NMSE improves by less than 0.5dB when the model's number of branches increases from 4 to 10 for a nonlinearity order of 9 or higher. Accordingly, having an automated criterion that selects the model dimensions (nonlinearity order and memory depth) based solely on its NMSE would lead to oversized models. This means that the model having the best NMSE will be selected even if a slightly worse NMSE can

be obtained from a model with significantly less coefficients. Conversely, if the model dimension information is included in the model assessment criterion, it is possible to select the model that achieves the best tradeoff between complexity evaluated in terms of the model's number of coefficients and accuracy expressed in terms of its NMSE. In this work, such criterion is implemented by adding, to the conventional NMSE metric, a penalty cost function that takes into account the model's number of coefficients. This complexity cost function is introduced to create a convexity in the model performance criterion since the NMSE cost function decreases while the complexity cost function increases as the model's number of coefficients increases. Accordingly, using the proposed hybrid model performance criterion will permit the automated selection of the model dimension which results in the best tradeoff between complexity and accuracy.

Thus, in order to choose the adequate memory polynomial model dimension that will achieve an acceptable trade-off between model accuracy and computational complexity, a novel criterion for the model performance evaluation is proposed.

For this, let us consider the memory polynomial model equation of (23) which can be re-written in a matrix form as follows:

$$y(n) = X(n)A \tag{47}$$

where $y(n)$ is the output complex baseband waveform of the model and $X(n)$ is defined as:

$$X(n) = [X_1 \ldots X_M] \tag{48}$$

and

$$X_j = [x(n+1-j)|x(n+1-j|^0 \ldots x(n+1-j)|x(n+1-j|^{N-1}], \ 1 \leq j \leq M$$

<div align="right">(49)</div>

The coefficients vector $\textbf{\textit{A}}$ is given by:

$$\textbf{\textit{A}} = \begin{bmatrix} a_{1,1} \ldots a_{1,M} \ldots a_{N,M} \end{bmatrix}^T$$

<div align="right">(50)</div>

Accordingly, the zero-norm of the coefficients vector $\textbf{\textit{A}}$ is:

$$\|\textbf{\textit{A}}\|_0 = \sum_{i=1}^{N} \sum_{j=1}^{M} \|a_{i,j}\|^0 = (M \times N)$$

<div align="right">(51)</div>

The minimization of the zero-norm is a technique that has been proposed in the literature for enforcing the sparsity in estimation problems [50, 51]. It is applied in this work to minimize the number of coefficients in the memory polynomial model. In order not to affect the accuracy of the model, a joint hybrid performance criterion that combines accuracy and complexity metrics is used. The accuracy is evaluated in terms of NMSE while the complexity is evaluated in terms of the number of coefficients or equivalently the zero-norm of the coefficients' vector $\textbf{\textit{A}}$. Since the NMSE is expressed in dB, the weighted dB value of the zero-norm is adopted. The zero-norm and the NMSE have a relation such that minimizing one ends up maximizing the other.

$$\min(zero-norm) \ \propto \ \max(NMSE)$$

<div align="right">(52)</div>

However, an optimum way of selecting a point of operation where both the zero-norm and NMSE are minimized as much as possible is needed. This is achieved only by developing another metric that comprises both the zero-norm and NMSE. Thus, the

hybrid criterion labeled complexity-aware-NMSE metric is expressed in dB and is stated as follows:

$$CAN_{dB} = NMSE_{dB} + \beta \times 10\log(\|\mathbf{A}\|_0)$$

$$= NMSE_{dB} + \beta \times 10\log(\sum_{i=1}^{N}\sum_{j=1}^{M}\|a_{i,j}\|^0)$$

$$= NMSE_{dB} + \beta \times 10\log(M \times N) \tag{53}$$

where the $NMSE_{dB}$ is the normalized mean squared error expressed in dB as defined in Equation (46). M and N are the number of branches and the nonlinearity order of the model, respectively. β is a weighting factor that is used to control the relative importance of each of the two parameters of the CAN metric and ranging from 0 to 0.2.

According to Equation (53) the CAN metric is made of the NMSE which reflects the model performance, and a model complexity cost function $(\beta \times 10\log(M \times N))$ that depends on the total number of coefficients in the model and thus, its complexity. According to Equation (51), the model's total number of coefficients is $(M \times N)$. It is worth mentioning here that the complexity cost function only depends on the total number of coefficients independently of the corresponding nonlinearity order and memory depth even though more than one pair of nonlinearity order and memory depth may lead to the same total number of coefficients. The weight of the cost function in the CAN metric is controlled by the value of β.

Figure 3.4 reports the model's complexity cost function versus the total number of its coefficients and a wide range of values for β. The curves reported in Figure 3.4 can be

used to select the value of the parameter β depending on the expected range for the model size and the relative importance of accuracy and complexity in the considered application. For instance, when a model is expected to have a large number of coefficients as it is the case in the conventional memory polynomial model, choosing a low value of β will not give any significant importance to the complexity cost function in the CAN metric. Conversely, if the memory polynomial has a reduced number of coefficients, it is more appropriate to select a reduced value for β. This choice should also take into account the admissible deviation between the model's NMSE and the minimal NMSE that can be achieved by selecting a model with a larger number of parameters. In this work, an NMSE deviation of up to 0.5dB is considered acceptable. Thus, according to the plots of Figure 3.4, the value of β was set to 0.17.
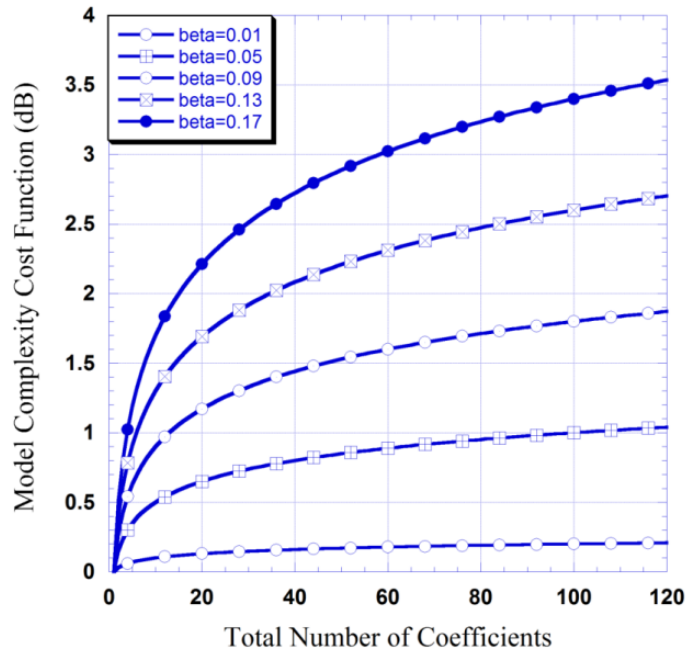
Figure 3.4 Model complexity cost function versus its total number of coefficients.

The CAN metric was calculated for the 100 models derived in the previous section using $\beta = 0.17$. The results are reported in Figure 3.5 which shows the calculated CAN metric as a function of the model's number of branches for different nonlinearity orders.
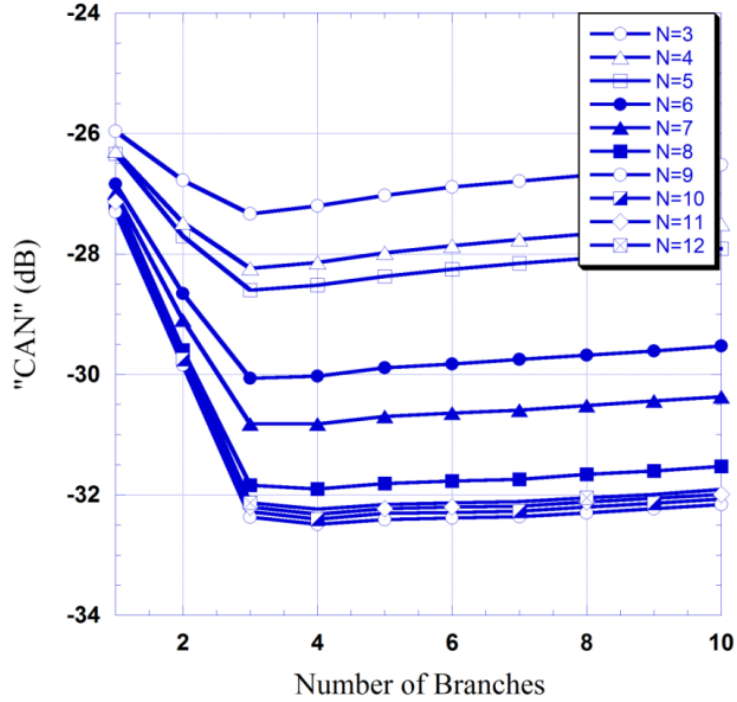
Figure 3.5 Complexity-aware NMSE of the memory polynomial model as a function of the model's number of branches for different nonlinearity orders.

Comparing the CAN results of Figure 3.5 with the NMSE results of Figure 3.3, one can see that the curves for nonlinearity orders exceeding 9 are not superimposed anymore. Moreover, the CAN metric plots have a convexity that is not observable in the NMSE plots. Based on the CAN metric, the best performance was obtained for $N = 9$ and $M = 4$, and corresponds to an NMSE of -35.5dB. This contrasts with the NMSE based dimension selection according to which the model dimension was found to be $N = 9$ and $M = 9$ for an NMSE of -35.9dB. Thus, the use of the proposed complexity-aware

NMSE reduced the number of coefficients in the model by 60% from 90 to 36 while "degrading" the NMSE by only 0.4dB.

To further validate the proposed metric and its ability to minimize the number of model coefficients without compromising its accuracy, a second device under test was used. The second DUT is a Gallium Nitride (GaN) based Doherty power amplifier designed for operation around 2140MHz. The detailed characteristics of this DUT are reported in [52]. This DUT was characterized using a long term evolution (LTE) signal having 20MHz bandwidth. Similarly to the validation carried out on the first DUT, several memory polynomial models were derived for the second DUT by sweeping the nonlinearity order from 3 to 12 and the number of branches from 1 to 10. For each of the identified models, the NMSE as well as the CAN metrics were calculated. The CAN metric was calculated for $\beta = 0.17$. The results, reported in Figure 3.6 for the NMSE criterion and Figure 3.7 for the CAN metric, corroborates the findings observed in the case of the first DUT. Indeed, according to the NMSE metric the best performance was obtained for $N = 9$ and $M = 10$ which resulted in a total of 90 coefficients. However, the use of the proposed CAN metric, the optimal parameters of the model were found to be $N = 9$ and $M = 3$. The model dimensions obtained using the CAN metric led to a model having 27 coefficients. This represents 70% reduction compared to the dimensions derived using the conventional NMSE metric. This significant reduction in the model complexity was achieved at the expense of a slight NMSE degradation from -40.6dB for the model having 90 coefficients to -40.1dB for the model having only 27 coefficients.

Figure 3.6 NMSE of the memory polynomial model of the second DUT as a function of the model's number of branches for different nonlinearity orders.
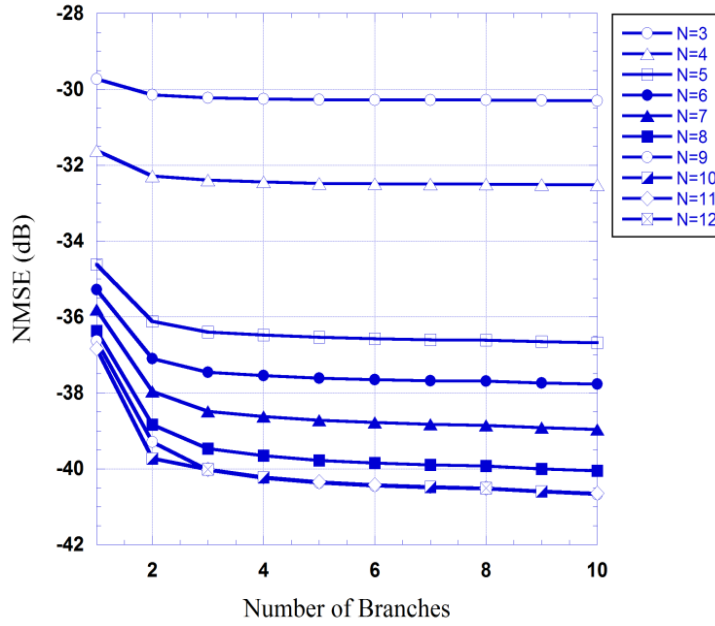

Figure 3.7 Complexity-aware NMSE of the memory polynomial model of the second DUT as a function of the model's number of branches for different nonlinearity orders.
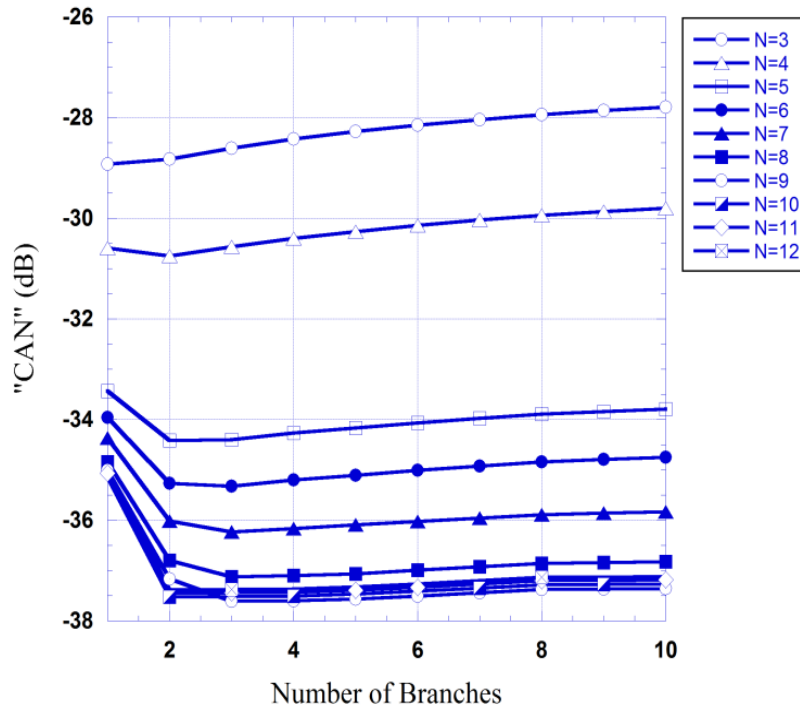
58

3.4 Case of the Twin-Nonlinear Two-Box Model

The proposed CAN metric can also be applied to determine the dimension of the memory polynomial function in two-box behavioral models. To investigate this, a 40MHz WCDMA signal was used to drive the amplifier. The measured input and output data were used to model the DUT using the forward twin-nonlinear two-box structure [7]. For each set of measurements, the LUT of the FTNTB model was identified once, and the input and output of the memory polynomial function de-embedded. Then, several memory polynomial functions were derived for different nonlinearity orders and memory depths. For this test, the nonlinearity order was swept from 1 to 5 and the number of branches was varied from 1 to 10. The nonlinearity order of the memory polynomial function was swept over a reduced range since the forward twin-nonlinear two-box structure inherently alleviates the need for high nonlinearity orders in the memory polynomial function [7]. The NMSE and CAN metrics were calculated for all model dimensions. The results, obtained for the first DUT, are reported in Figure 3.8 (a) for the NMSE and Figure 3.8 (b) for the CAN. These results are inline with those observed in the case of the conventional memory polynomial model. Indeed, the use of the NMSE criterion led to a model having 50 coefficients ($N = 5$ and $M = 10$) with a NMSE of -36.0 dB. However, the use of the CAN metric resulted in a model having only 20 coefficients ($N = 5$ and $M = 4$) with an NMSE of -35.7dB. This further demonstrates the ability of the proposed approach in automatically selecting the model dimension without compromising the model accuracy. In fact, for the forward twin-nonlinear two-box

model, a 60% reduction in the number of coefficients was obtained while the NMSE was

degrades by less than 0.5dB.
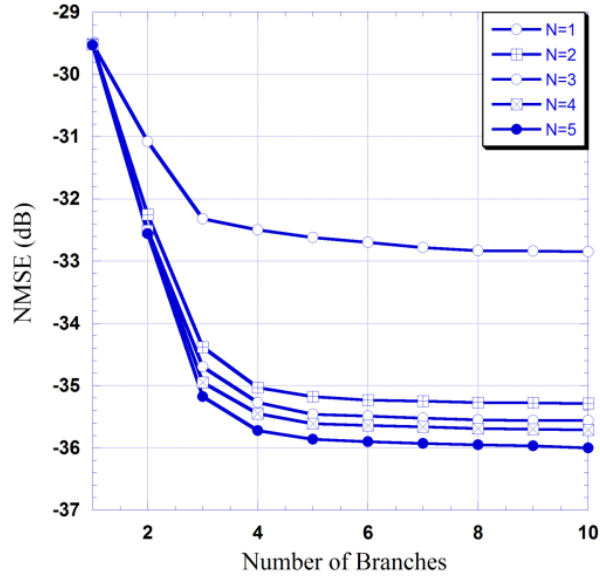
(a)
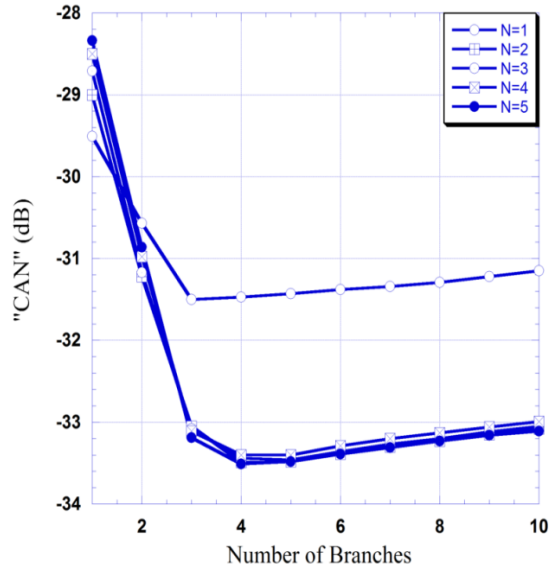
(b)

Figure 3.8 Performance of the forward-twin nonlinear two-box model as a function of the memory polynomial's number of branches and nonlinearity order. (a) NMSE, (b) Complexity-aware NMSE.

The second DUT was also used to further validate the proposed CAN metric in the context of the forward twin-nonlinear two-box model. The nonlinearity order and number of branches of the memory polynomial function were swept from 1 to 5 and from 1 to 10, respectively. For each model, the NMSE and CAN metrics were calculated. According to the obtained results reported in Figure 3.9 (a) for the NMSE and Figure 3.9 (b) for the CAN metric, the use of the NMSE criterion for the model dimension selection led to a model having 50 coefficients with nonlinearity order $N = 5$ and number of branches $M = 10$. However, the model dimension selected using the CAN criterion was 4 coefficients with $N = 1$ and $M = 4$. Thus, determining the size of the forward twin-nonlinear two-box model's polynomial function using the CAN metric allowed for reducing the memory polynomial's number of coefficients from 50 to 4 while changing the model's NMSE from -41.1dB to -40.2dB.
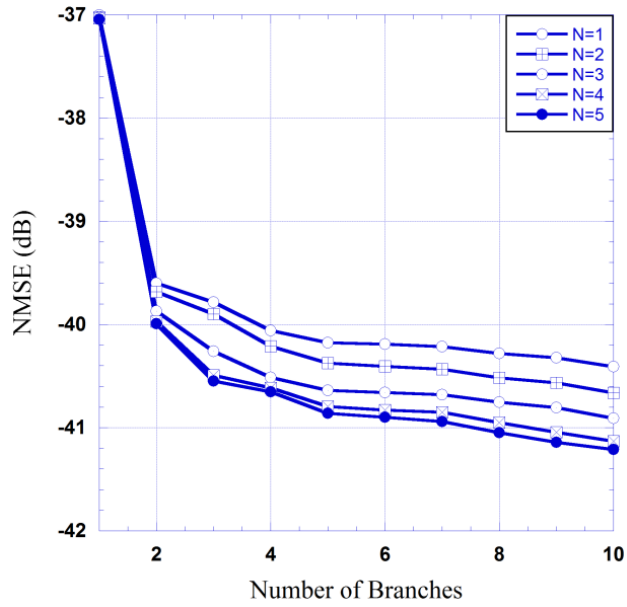
(a)
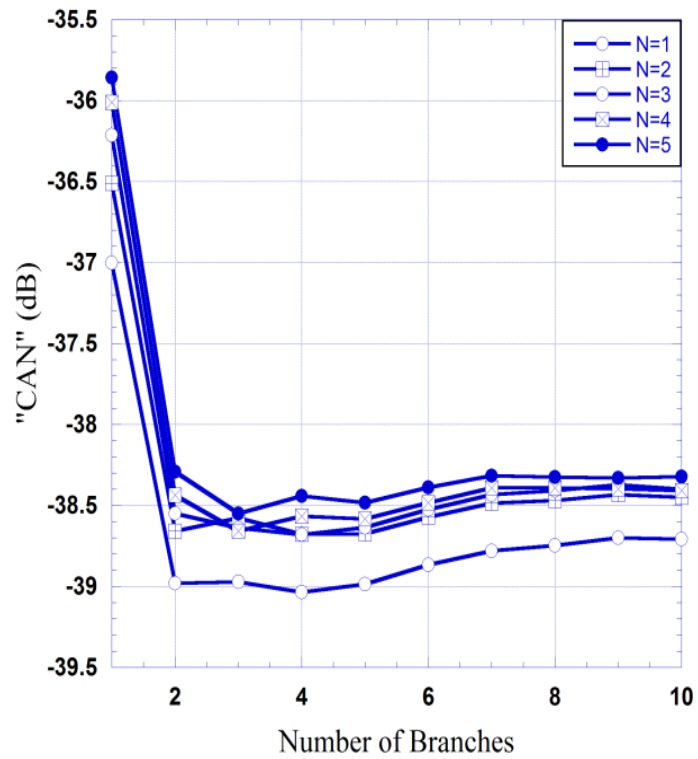
(b)

Figure 3.9 Performance of the forward-twin nonlinear two-box model of the second DUT as a function of the memory polynomial's number of branches and nonlinearity order. (a) NMSE, (b) Complexity-aware NMSE.

3.5 Summary

In this chapter, a complexity-aware-NMSE metric was proposed for determining the dimension of the memory polynomial function in power amplifiers behavioral models. The proposed metric takes into account both the performance of the model and its number of coefficients in order to select the dimension that achieves a trade-off between accuracy and complexity. The proposed metric was applied for the modeling, using the conventional memory polynomial and the forward-twin-nonlinear two-box models, of a two Doherty power amplifiers driven by wideband signals. The results show that, compared to the conventional approach that uses the NMSE, the proposed technique significantly reduces the model dimension while maintaining its accuracy.

CHAPTER 4

BANDWIDTH SCALABLE BEHAVIOURAL MODELS

FOR POWER AMPLIFIERS WITH MEMORY

In this chapter, generic bandwidth-scalable behavioral modeling suitable for power amplifiers exhibiting memory effects is proposed. Such models are built around state of the art two-box models, namely the Hammerstein model and the forward twin-nonlinear two-box (FTNTB) model, and take advantage of the separation, in these two-box models, between the static and dynamic distortions of the power amplifier. In the proposed bandwidth-scalable two-box models, rather than updating the entire model coefficients when the signal bandwidth changes, the memoryless function is maintained unchanged and only the function modeling the dynamic distortions is updated. Experimental validations carried out on a Doherty and Class AB amplifier prototypes show that the proposed bandwidth-scalable models are able to achieve the same performance as the conventional models while reducing the number of coefficients to be updated following a change in the operating signal bandwidth by up to approximately 75% for the Hammerstein model and 40% for the FTNTB model. The developed models are suitable for emerging wireless applications where operating conditions vary rapidly.

4.1. Motivation

Radio frequency power amplifiers are the main source of nonlinearity in wireless transmitters. This nonlinear behavior is unavoidable in modern applications due to the high peak-to-average power ratio of the used signals which will result in very low power efficiency in linear mode of operation. Thus, it is important to model the nonlinear behavior of the power amplifier in order to predict its performance and evaluate its linearizability.

Various behavioral models with two-box structures mainly built around the memory polynomial functions that were discussed in literature review [6]. One of the major limitations of the models proposed so far is that their coefficients are valid for a specific set of operating conditions defined mainly by the signal's average power, its bandwidth, and to a lesser extent its statistics. This means that to maintain the accuracy and performance of a model, its parameters and/or coefficients need to be updated whenever the input signal characteristics change. In [53], the reverse twin-nonlinear two-box model was successfully applied for the synthesis of scalable digital predistorter. In this chapter, a scalable behavioral model based on the forward twin-nonlinear two-box and the Hammerstein structures is reported. The proposed model introduces some scalability in behavioral models to reduce the complexity associated with the model update following a change in the input signal characteristics. This work exclusively focuses on bandwidth variations of the input signal. It exploits the separation in two-box models between the static and dynamic distortions and the fact that the static distortions are mainly impacted by the signal's average power and statistics while being quasi-insensitive to the signal's

bandwidth. Thus, in the proposed bandwidth-scalable two-box models, the static distortions (memoryless AM/AM andAM/PM functions) are determined from measurements under quasi-memoryless operating condition using narrowband signals [64]. When the signal bandwidth is varied, the static distortions are maintained unchanged and only the dynamic distortions are updated. This approach is experimentally validated on a 300-Watt Doherty power amplifier driven by signals with up to 40MHz bandwidth. The results clearly show that the proposed approach significantly reduces the number of coefficients to be updated and leads to the same performance as the conventional versions of the same two-box models.

The rest of the chapter is organized as follows: in section 4.2, the experimental setup is described. In Section 4.3, the proposed bandwidth scalable behavioral model is introduced where the static distortions and dynamic distortions are identified separately. In Section 4.4, the proposed model is benchmarked against the conventional Hammerstein and forward twin-nonlinear two-box models.

4.2. Experimental Setup

The measurements used in this chapter were performed at the intelligent RF radio technology (iRadio) laboratory at the electrical and computer engineering department of the university of Calgary, Alberta, Canada. The experimental setup used in this work is shown in Figure 4.1. The DUTs were characterized using the input and output complex baseband waveforms. The arbitrary waveform generator generates the RF signal that drives the power amplifier prototypes. The power amplifier prototypes used are the Doherty and Class AB. The RF output signal is collected at the other end of the DUT

with a vector signal analyzer (VSA). During the cases of high power amplifiers, it is customary to apply attenuation before it is directly connected to VSA to adjust to its input power requirement. Both the input generated signals and the amplified output signals are recorded by the data processing software loaded in a work station computer via the local area network (LAN) or GPIB interfaces.
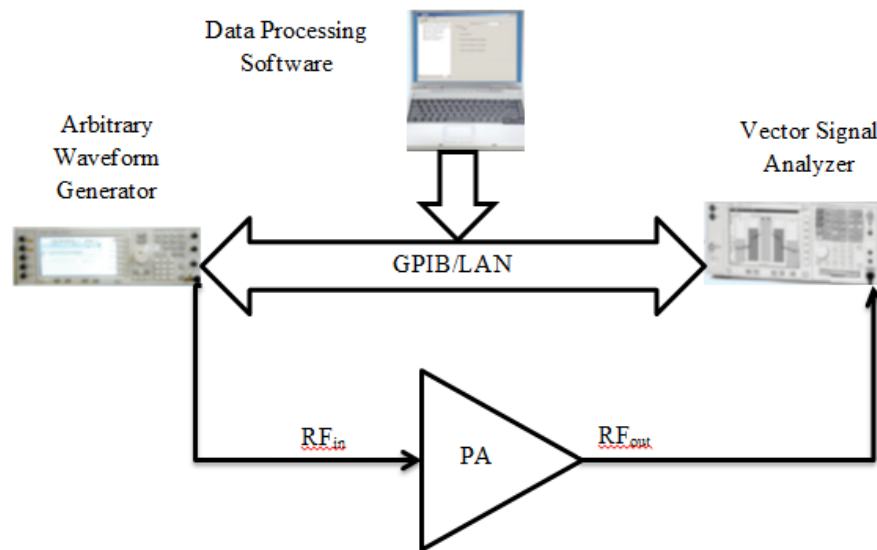
Figure 4.1 Experimental setup for the device under test [6]

The first DUT used for the experimental validation is a 300-Watt Doherty power amplifier operating in the 2110-2170MHz frequency band. The test signals were carefully designed in order to solely observe the signal's bandwidth effects on the behavior of the device under test. Thus, a WCDMA digital waveform was first synthesized. This signal has a bandwidth of 5MHz and a PAPR of 10dB. Then, to generate test signals that only differ from the original signal by their bandwidths, the original waveform was sampled at a higher clock rate in order to increase the bandwidth of the signal while maintaining its

peak-to-average power ratio and its statistics unchanged. Signal bandwidths that are 6 and 8 times wider than the original WCDMA signal were generated and used to characterize the device under test.

The AM/AM and AM/PM characteristics of the device under test were measured using the instantaneous input and output complex baseband waveform technique. However, since the bandwidths involved (up to 40MHz and 200MHz for the input and output signals, respectively) cannot be handled by commercial vector signal analyzers, a custom designed transmitter and receiver chains were used [60].

A general system identification procedure is stated in [54]. However, for the bandwidth scalable behavioral modeling and all the power amplifier model identification procedure is indicated in Figure 4.2. Key steps from measurement to model validation are shown. The first step is to get the baseband complex waveforms from the measurement setup that is shown in Figure 4.1. A delay estimation and adjustment should be handled before model identification so that to compensate for the propagation delay through DUT which introduces a mismatch between the data samples of the input and output. This mismatch will be represented as dispersion in the AM/AM and AM/PM characteristics which can be misinterpreted as memory effects. The resolution needed for the delay compensation is usually lower than the signal sampling rate. Thus, signal up-sampling and down-sampling is required during delay estimation and compensation process. The time delay compensated input and output signal waveforms are used in the model identification and performance analyzing steps.
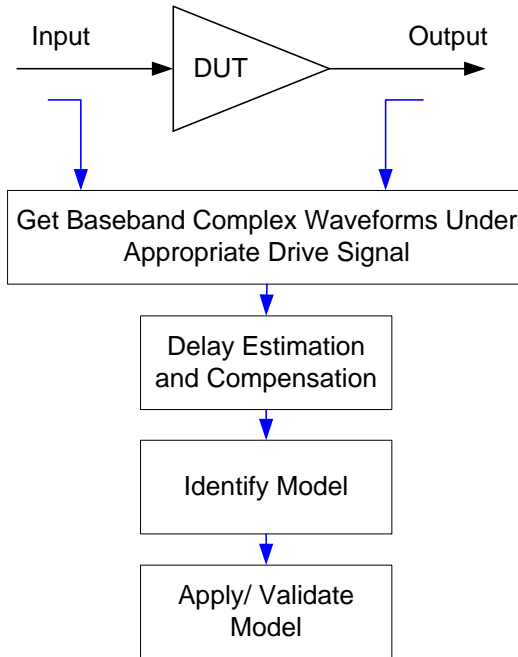
Figure 4.2 Behavioral model extraction procedure [6]

The number of coefficients of the model is also considered in the model identification step. This thesis work consists of a contribution in regard to choosing appropriate optimum model parameters by ensuring enough degree of freedom to describe the full range of behavior of the amplifier without affecting the performance. After choosing the model and the identification algorithm, the model coefficients can be extracted from measurement input-output data.

The model validation stage which involves various procedures to evaluate how the model behaves for the intended application [55]. The models that we are going to be discussed in the coming sections pass through this model extraction process that is shown in Figure 4.2. The next section will further elaborate the bandwidth scalable models and approach.

4.3. Proposed Models and Approach

The proposed models are inspired from the Hammerstein and the FTNTB models [6, 7, 56]. Both of these two-box models are built using a memoryless nonlinear function, modeling the static distortions, followed by a cascaded function that models the dynamic distortions. Such architectures have one major advantage that can be beneficially used to build the proposed bandwidth-scalable behavioral models. Indeed, the static distortions and dynamic distortions are identified separately. This is an important property that distinguishes these models from other structures such as the memory polynomial or the nested look-up table models in which there is no separation between the static and dynamic distortions [57, 58]. Commonly, the memoryless nonlinear function modeling the static distortions is obtained by processing the input and output baseband waveforms measured for the operating signal which might have any bandwidth. However, it has been shown, in [59], that when the signal bandwidth gets wider, the estimated static distortions are affected by the presence of memory effects and thus the "true" memoryless characteristic of the device under test (DUT) is that measured using a narrowband signal which does not emulate memory effects. Based on this, the memoryless characteristic of the proposed models is forced to be bandwidth independent and is not updated / recalculated when the bandwidth of the test signal is varied. Only the second box, which is used to model the dynamic distortions, is updated following changes in the signal bandwidth. This is a major contrast with previously reported models where the entire model (including both functions) needs to be updated following any changes in the

operating signal bandwidth. The proposed generic structure for bandwidth-scalable behavioral models is presented in Figure 4.3 (a). It is made of the cascade of bandwidth-independent static distortions and bandwidth-dependent dynamic distortions. Figure 4.3 (b) illustrates how this structure can be used to build the bandwidth-scalable FTNTB model.
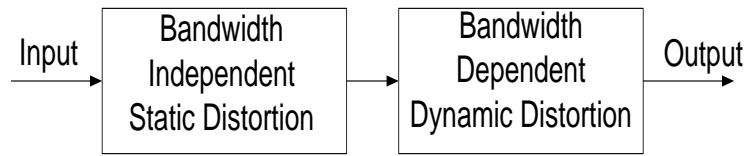
(a)
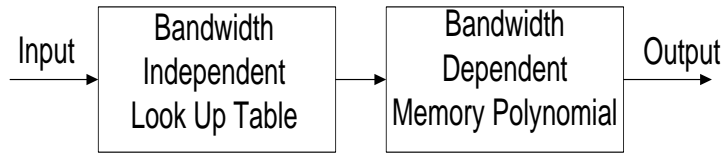
(b)

Figure 4.3 The proposed generic bandwidth-scalable two-box models. (a) generic structure, (b) application to the bandwidth scalable FTNTB model

Figure 4.4 represents the memoryless AM/AM and AM/PM characteristics of the device under test measured for the different test signals. This clearly shows that, as expected, the static distortions are quasi-insensitive to the signal bandwidth. The slight variations are mainly due to the impact of memory effects on the averaging of the measured data. Similar behavior is observed for the AM/PM characteristics.
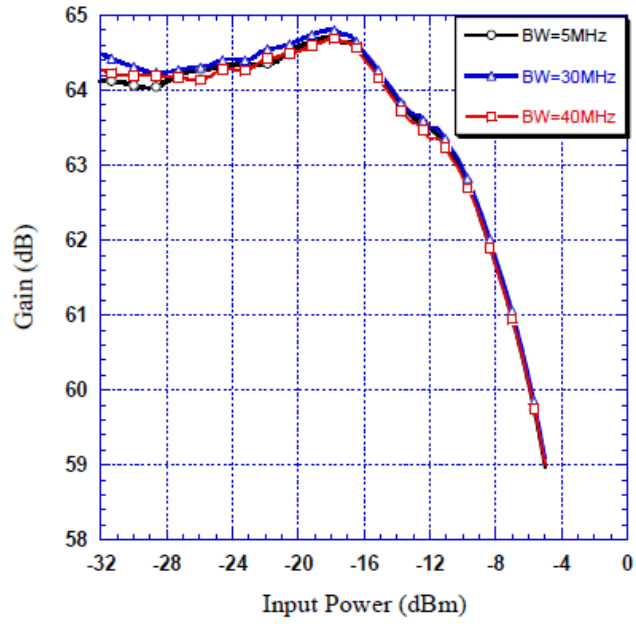
(a)
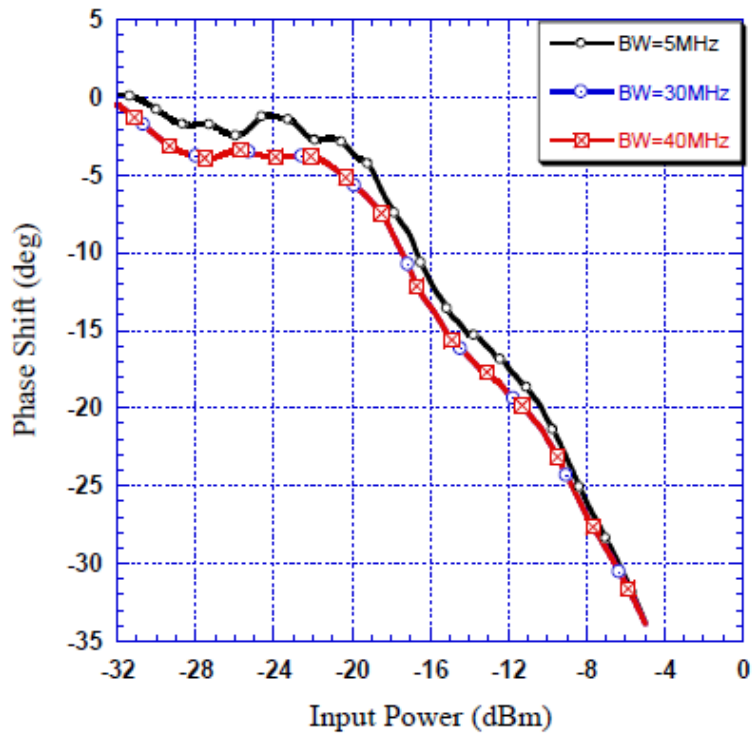
(b)

Figure 4.4. Measured memoryless characteristics of the DUT for signal bandwidths of 5MHz, 30MHz, and 40MHz. (a) AM/AM characteristic, (b) AM/PM characteristic

4.4. Benchmarking Against Conventional Models

In this section, the performances of the proposed generic bandwidth-scalable behavioral models are benchmarked against the performance of their corresponding conventional counterparts. Thus, the proposed bandwidth-scalable Hammerstein model (where the static nonlinear function is made bandwidth-independent) is compared to the conventional Hammerstein model (where the static nonlinear function is bandwidth-dependent). Similarly, the bandwidth-scalable FTNTB model is compared to its conventional version.

First the conventional Hammerstein and FTNTB models were identified. For both models, the memory depth was set to 4 for the 30MHz wide signal, and 5 for the 40MHz wide signal. For the FTNTB model, the nonlinearity order of the memory polynomial function modeling the dynamic distortions was set to 5 for both signals for the first DUT and set 6 for both the signals for second DUT. Then, the bandwidth-scalable models having the same sizes as their conventional counterparts were identified. For these models, the static distortions characteristics used were that measured using the 5MHz test signal. Table 4.1 reports the calculated NMSE for the four models. These results show that for both structures (the Hammerstein and the FTNTB models), the conventional and the bandwidth-scalable versions lead to comparable NMSE performance for both test signals. This clearly shows that the proposed approach does not lead to any degradation in the model performance. To further investigate this, the memory depth of the models was varied from 1 to 10 and the nonlinearity order of the memory polynomial function

used in the FTNTB model was varied from 1 to 6. For each set of dimensions, the conventional and bandwidth-scalable models were derived, and the NMSE variation was calculated for each set of nonlinearity order and memory depth according to:

$$\Delta NMSE = |NMSE_{conventioal} - NMSE_{BandwidthScalable}| \qquad (54)$$

where $NMSE_{conventioal}$ and $NMSE_{BandwidthScalable}$ are the NMSE calculated for the conventional and the bandwidth-scalable models, respectively.

The results collected on the two DUTs show that the NMSE variations do not exceed 0.25dB and 0.5dB for Doherty PA and Class AB PA, respectively. The NMSE results, shown in Table 4.1 and Table 4.2, indicate that both the conventional and bandwidth scalable models lead to similar performance.

As of Table 4.1, the conventional Hammerstein model for the Doherty PA where the filter and the nonlinear boxes are identified using the 30MHz and 40MHz signals results in NMSE value of -32.74dB and -32.61dB, respectively. Conversely, the proposed bandwidth scalable Hammerstein model, where the bandwidth independent nonlinearity box is identified using a 5MHz signal and bandwidth dependent dynamic part is represented as a filter is identified using 30MHz and 40MHz signal, results in NMSE value of -32.68dB and -32.57dB. The average NMSE variation between the conventional and proposed Hammerstein modes is 0.05dB NMSE.

Table 4.1 Comparison between the NMSE of the conventional and bandwidth scalable models of the Doherty PA

		Signal Bandwidth	
Models		30MHz	40MHz
Hammerstein	Conventional	-32.74dB	-32.61dB
	Bandwidth Scalable	-32.68dB	-32.57dB
FTNTB	Conventional	-34.82dB	-35.80dB
	Bandwidth Scalable	-34.77dB	-36.04dB

On the other hand, the conventional FTNTB for the Doherty DUT model where the LUT and the memory polynomial boxes are identified both using the 30MHz and 40MHz signals results in NMSE value of -34.82dB and -35.80dB, respectively. However, the proposed bandwidth scalable FTNTB models have the NMSE value of -34.77dB and -36.04dB when 30MHz and 40MHz signals are used respectively. The NMSE variation of 0.05dB is observed when a 30MHz driving signal is used. However, it has been observed an NMSE improvement of 0.24dB for the proposed scalable model as it is compared to the conventional method when the DUT is driven by 40MHz signal. Therefore the average NMSE variation between the conventional and proposed method on based on FTNTB model is 0.15dB.

As of Table 4.2, the conventional Hammerstein model for second DUT driven by 30MHz and 40MHz signals results in NMSE value of -33.6dB and -33.2dB respectively while the proposed bandwidth scalable Hammerstein model results in NMSE value of -33.1dB and -32.8dB respectively. The average NMSE variation between the conventional and proposed Hammerstein modes is 0.5dB NMSE.

Table 4.2 Comparison between the NMSE of the conventional and bandwidth scalable models of the class AB PA

Models		Signal Bandwidth	
		30MHz	40MHz
Hammerstein	Conventional	-33.6 dB	-33.2 dB
	Bandwidth Scalable	-33.1 dB	-32.8 dB
FTNTB	Conventional	-35.3 dB	-35.4 dB
	Bandwidth Scalable	-35.0 dB	-35.4 dB

Table 4.2 also consists of the results of FTNTB model based comparison of the conventional and proposed method for the class AB DUT when driven by the same 30MHz and 40MHz signals. The FTNTB model results in the NMSE values of -35.3dB and -35.4dB for the 30MHz and 40MHz test signals, respectively. The scalable version of this model results in NMSE of -35.0dB and -35.4dB for the 30MHz and 40MHz test signals, respectively. This indicates that for the 40MHz signal, the proposed bandwidth scalable modeling technique achieves the same performance as that of the conventional modeling approach while for 30MHz signal 0.3dB variation is observed. The average variation in the NMSE value between the conventional and the bandwidth scalable based on the FTNTB model is 0.15dB.

To evaluate the gain in complexity reduction achieved by using the proposed bandwidth-scalable models, the number of coefficients to be updated in each model will be considered. The static nonlinear function in two-box models is commonly implemented using a look-up table, yet it can be considered as a polynomial function of order (K). The function modeling the dynamic distortions is a simple finite impulse response (FIR) filter

of order M for Hammerstein models and a memory polynomial function of size M × N

for the twin-nonlinear two-box model. Herein, M represents the memory depth and N is

the nonlinearity order of the polynomial function used in the TNTB models.

Thus, the total number of parameters (S) of the model is

$$S = K + (N \times (M + 1)) \tag{55}$$

where $N = 1$ for the Hammerstein model

Accordingly, in the proposed bandwidth-scalable behavioral models, the number of

coefficients that will be updated is (M + 1) for the Hammerstein model, and (N × (M +

1)) for the FTNTB model.

Typically, K in (55) ranges between 10 and 14 for the DUTs. An average value of 12 was

used to estimate the number of coefficients needed for the static nonlinear function of all

models. The number of coefficients that needs to be updated once the signal bandwidth is

changed from 5MHz to 30MHz and 40MHz are reported in Table 4.3 and Table 4.4.

Table 4.3 presents a comparison between the conventional and the proposed methods in

terms of total number of model coefficients to be updated for the Doherty PA.Based on

the Hammerstein model, bandwidth-scalable modeling results in the reduction of 75%

and 70.5% in total number of parameter when the DUT is driven by 30MHz and 40MHz

signal, respectively. The reduction of 37.5% and 32.4 % in total number of coefficients to

be updated are achieved when the bandwidth-scalable modeling is implemented on the

FTNTB model for 30MHz and 40MHz driving signals, respectively. Thus, the average

total number of parameter reduction for the Hammerstein and FTNTB based bandwidth-scalable modeling is 72.3% and 35%, respectively.

Table 4.3 Number of coefficients to be updated for the conventional and the bandwidth-scalable models for Doherty PA

		Signal Bandwidth	
Models		30MHz	40MHz
Hammerstein	Conventional	16	17
	Bandwidth Scalable	4	5
FTNTB	Conventional	32	37
	Bandwidth Scalable	20	25

The result of a similar analysis that was carried out on the class AB DUT is presented in Table 4.4. This table shows the comparison between the conventional and proposed models' total number of coefficients to be updated in the Hammerstein and the FTNTB models. The results based on Hammerstein models show that the proposed method achieves a reduction in the number parameters by 75% and 70.5% when the DUT is driven by 30MHz and 40MHz signals, respectively. Total reduction of 33.3% and 28.6 % in total number of coefficients to be updated are noticed when the bandwidth-scalable modeling is implemented on the FTNTB model for 30MHz and 40MHz driving signals, respectively. In summary, the average reduction for the Hammerstein and FTNTB based bandwidth-scalable modeling is 72.25% and 31% respectively.

Table 4.4 Number of parameters to be updated for the conventional and the bandwidth scalable models for class AB PA

Models		Signal Bandwidth	
		30MHz	40MHz
Hammerstein	Conventional	16	17
	Bandwidth Scalable	4	5
FTNTB	Conventional	36	42
	Bandwidth Scalable	24	30

4.5.   Summary

Hence, in summary the bandwidth-scalable Hammerstein model reduces the number of coefficients to be updated by 70% to 75%, while the complexity reduction is in the range of 29% to 45% for the bandwidth scalable FTNTB model. It can be seen from (55) that as the memory effects present in the DUT decrease, the complexity reduction gained by the use of the proposed bandwidth-scalable models increases.

CHAPTER 5

CONCLUSION

A complexity-aware-NMSE metric was proposed for determining the dimension of the memory polynomial function in power amplifiers behavioral models. The metric takes into account both the performance of the model and its number of coefficients in order to select the dimension that achieves a trade-off between accuracy and complexity. The proposed metric was applied for the modeling, using the conventional memory polynomial and the forward-twin-nonlinear two-box models, of a high power Doherty amplifier driven by a wideband signal. The proposed method was verified on using an LDMOS and a GaN based power amplifiers. The results showed that, compared to the conventional approach that uses the NMSE, the proposed technique reduces by up to 60% the model dimension while maintaining its accuracy.

Moreover, novel bandwidth-scalable behavioral models for RF power amplifiers exhibiting memory effects were reported. The proposed models were implemented based on Hammerstein and FTNTB models. The experimental validations, that are performed using two DUTs, demonstrated the effectiveness of the proposed models. Indeed, they maintain the same performance as their conventional counterparts but with a significantly lower number of coefficients that need to be updated following a change in the bandwidth of the amplifier's drive signal. The bandwidth-scalable models set the ground for the development of a new class of behavioral models suitable for emerging standards and that can be easily adapted to variations in the input signal characteristics.

As a future work, the complexity aware metric technique could be extended to other metric in the frequency domain. One of such metrics can be the normalized average mean spectrum error (NAMSE). NAMSE considers the error in frequency domain between the measured and model output as NMSE does in the time domain. Thus, NAMSE could be an ideal choice to further extend to develop and validate the metric into being complexity aware in frequency domain. Moreover, the work of the bandwidth-scalable modeling that was reported in chapter 4 could be extended by applying the scalable technique on other models such as DDR and PLUME models. These models could be suitable because of their structures in separating the static and dynamic nonlinearities of the system and their performance.

Appendix - Impedance Calculation

The impedance of quarter wave transmission line with respect to the impedance of the load in the Doherty power amplifier circuit is shown at the following figure.
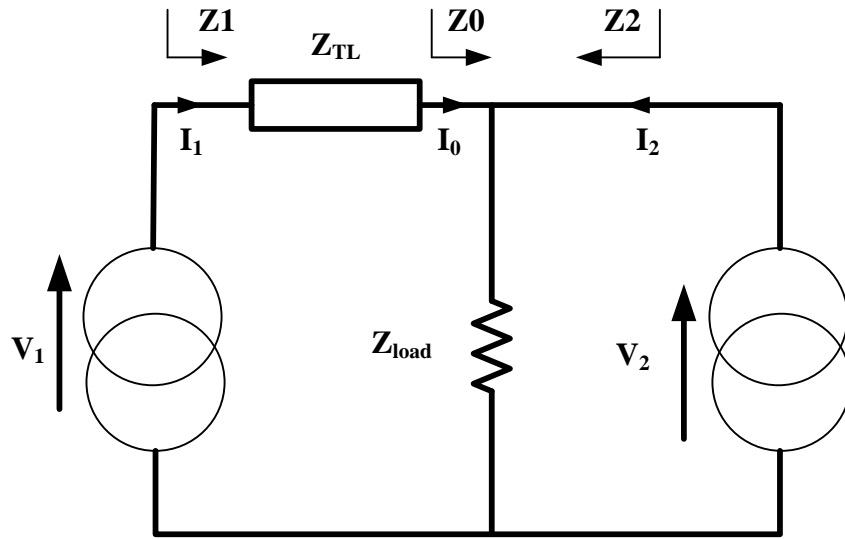
Applying the load modulation,

$$Z_0 = Z_{load}\left(1 + \frac{I_2}{I_0}\right) \tag{56}$$

$$Z_2 = Z_{load}\left(1 + \frac{I_0}{I_2}\right) \tag{57}$$

The quarter wave transmission line can be stated as

$$Z_{TL} = \sqrt{Z_1.Z_0} \tag{58}$$

$$Z_{TL}^2 = \frac{V_1}{I_1}\frac{V_2}{I_0} \tag{59}$$

Since $V_1 I_1 = V_2 I_0$

$$I_0 = \frac{V_1}{Z_{TL}} \tag{60}$$

When I_0 is substituted

$$Z_0 = Z_{load}\left(1 + \frac{I_2}{I_0}\right) = Z_{load}\left(1 + \frac{I_2 Z_{TL}}{V_1}\right) \tag{61}$$

$$Z_{TL} = \sqrt{Z_1 . Z_0} = \sqrt{Z_1 . Z_{load}\left(1 + \frac{I_2 Z_{TL}}{V_1}\right)} \tag{62}$$

$$Z_1 = \frac{Z_{TL}^2}{Z_{load}\left(1 + \frac{I_2 Z_{TL}}{V_1}\right)} \tag{63}$$

Thus, the output voltage of the main amplifier can be represented as follows

$$V_1 = I_1 Z_1 = \frac{I_1 Z_{TL}^2}{Z_{load}\left(1 + \frac{I_2 Z_{TL}}{V_1}\right)} \tag{64}$$

Assuming "n" having a value ranging from 0 to 1 in the 6dB back off range in terms of maximum current, $I_{max}/2$

$$I_1 = \frac{I_{max}}{2}(1 + n) \tag{65}$$

$$I_2 = \frac{I_{max}}{2}n \tag{66}$$

when we substitute the current values of I_1 and I_2 into the last formulation of V_1

$$V_1 = \frac{I_{max} Z_{TL}}{4 Z_{load}}\left(Z_{TL} + n(Z_{TL} - 2Z_{load})\right) \tag{67}$$

Efficiency enhancement is achieved when V_1 is constant in the 6 dB back off region. Thus, it needs to be independent of 'n'. The above equation can be simplified as

$$Z_{TL} = 2Z_{load} \qquad (68)$$

The 6 dB back off region is considered as the operation point of the Doherty power amplifier. The efficiency comparison plot the Doherty and class AB power amplifiers are presented in the Figure A.1. The solid line represented the efficiency vs input signal power of the Doherty while the broken line represents that of the class AB.
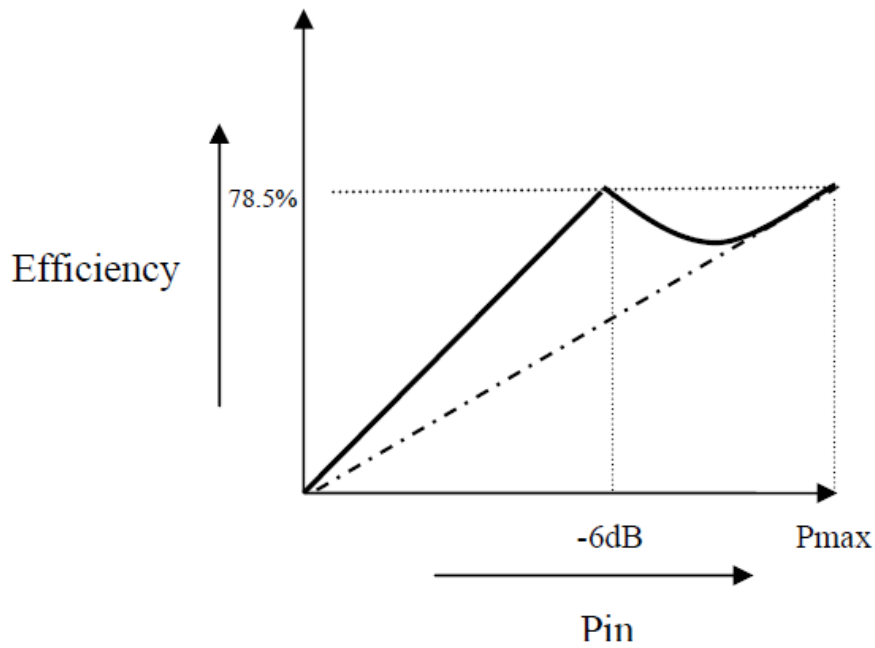
Figure A.1 Efficiency plot of Doherty and class AB power amplifiers

References

[1]   ETSI, "Environmental Engineering Measurement Method for Energy Effeciency of Wireless Access Network Equipment," 2011-10.

[2]   G. Proakis and M. Salehi, "Digital Communications," *McGraw-Hill International Edition,* 2008.

[3]   R. Giofre, P. Colantonio, and F. Giannini, "GaN broadband Power Amplifiers for terrestrial and space transmitters," *19th International Conference on Microwave Radar and Wireless Communications (MIKON),* vol. 2, pp. 605-609, 2012.

[4]   B. Kim, I. Kim, and J. Moon, "Advanced Doherty Architecture," *IEEE Microwave Magazine,* vol. 11, pp. 72-86, 2010.

[5]   S. C. Cripps, *RF power amplifiers for wireless communications, second edition*: Artech House, Incorporated, 2006.

[6]   F. M. Ghannouchi and O. Hammi, "Behavioral modeling and predistortion," *Microwave Magazine, IEEE,* vol. 10, pp. 52-64, 2009.

[7]   O. Hammi and F. M. Ghannouchi, "Twin Nonlinear Two-Box Models for Power Amplifiers and Transmitters Exhibiting Memory Effects With Application to Digital Predistortion," *IEEE Transactions on Microwave and Wireless Components Letters,* vol. 19, pp. 530-532, 2009.

[8]   A. Zhu, J. C. Pedro, and T. J. Brazil, "Dynamic Deviation Reduction-Based Volterra Behavioral Modeling of RF Power Amplifiers," *IEEE Transactions on Microwave Theory and Techniques,* vol. 54, pp. 4323-4332, 2006.

[9]   F. Taringou, O. Hammi, B. Srinivasan, Malhame, x, R., and F. M. Ghannouchi, "Behaviour modelling of wideband RF transmitters using Hammerstein-Wienermodels," *Circuits, Devices & Systems, IET,* vol. 4, pp. 282-290, 2010.

[10]   R.K . Pearson, "Selecting nonlinear model structures for computer control," *J. Process Control,* vol. 13, pp. 1-26, 2003.

[11]   V. Z. Marmarelis, "Nonlinear Dynamic Modeling of Physiological Systems," *John Wiley and Sons,* 2004.

[12]   W. J. Rugh, "Nonlinear System Theory, the Volterra/Wiener Approach," *Johs Hopkins University Press,* 1981.

[13]   R. Raich, Q. Hua, and G. T. Zhou, "Orthogonal polynomials for power amplifier modeling and predistorter design," *IEEE Transactions on Vehicular Technology,* vol. 53, pp. 1468-1479, 2004.

[14]   D. R. Morgan, M. Zhengxiang, K. Jaehyeong, M. G. Zierdt, and J. Pastalan, "A Generalized Memory Polynomial Model for Digital Predistortion of RF Power Amplifiers," *IEEE Transactions on Signal Processing,* vol. 54, pp. 3852-3860, 2006.

[15]   R. N. Braithwaite, "Wide bandwidth adaptive digital predistortion of power amplifiers using reduced order memory correction," in *Microwave Symposium Digest, 2008 IEEE MTT-S International*, 2008, pp. 1517-1520.

[16]   A. Kwan, O. Hammi, M. Helaoui, and F. M. Ghannouchi, "High performance wideband digital predistortion platform for 3G+ applications with better than

55dBc over 40 MHz bandwidth," in *IEEE MTT-S International Microwave Symposium Digest (MTT)*, 2010, pp. 1082-1085.

[17] W. Huang-Jie, X. Jing, Z. Jian-Feng, T. Ling, Y. Meng-Su, Z. Lei, and Z. Xiao-Wei, "A wideband digital pre-distortion platform with 100 MHz instantaneous bandwidth for LTE-advanced applications," in *2012 Workshop on Integrated Nonlinear Microwave and Millimetre-Wave Circuits (INMMIC)* 2012, pp. 1-3.

[18] G. Lei and Z. Anding, "Simplified dynamic deviation reduction-based Volterra model for Doherty power amplifiers," in *2011 Workshop on Integrated Nonlinear Microwave and Millimetre-Wave Circuits (INMMIC)*, 2011, pp. 1-4.

[19] Z. Anding and J. C. Pedro, "Distortion Evaluation of RF Power Amplifiers Using Dynamic Deviation Reduction Based Volterra Series," in *IEEE/MTT-S International Microwave Symposium, 2007*, 2007, pp. 965-968.

[20] J. Kim and K. Konstantinou, "Digital predistortion of wideband signals based on power amplifier model with memory," *Electronics Letters,* vol. 37, pp. 1417-1418, 2001.

[21] H. Sungchul, W. Young Yun, K. Jangheon, C. Jeonghyeon, K. Ildu, M. Junghwan, Y. Jaehyok, and B. Kim, "Weighted Polynomial Digital Predistortion for Low Memory Effect Doherty Power Amplifier," *IEEE Transactions on Microwave Theory and Techniques* vol. 55, pp. 925-931, 2007.

[22] F. Kai, C. L. Law, G. Cunfeng, T. Than Tun, and K. Myat Thu, "A new power amplifier predistortion architecture based on memory polynomial model," in *Information, Communications and Signal Processing, 2009. ICICS 2009. 7th International Conference on*, 2009, pp. 1-5.

[23] M. Rawat, F. M. Ghannouchi, and K. Rawat, "Three-Layered Biased Memory Polynomial for Dynamic Modeling and Predistortion of Transmitters With Memory," *IEEE Transactions on Circuits and Systems I: Regular Papers,* vol. 60, pp. 768-777, 2013.

[24] M. Abi Hussein, V. A. Bohara, and O. Venard, "Two-dimensional memory selective polynomial model for digital predistortion," in *IEEE 10th International New Circuits and Systems Conference (NEWCAS)*, 2012, pp. 469-472.

[25] S. Bachir, C. Duvanaud, and M. Djamai, "On-line memory polynomial predistortion based on the adapted kalman filtering algorithm," in *Joint 6th International IEEE Northeast Workshop on Circuits and Systems and TAISA Conference, NEWCAS-TAISA*, 2008, pp. 65-68.

[26] C. Gang, T. Xu, L. Taijun, Y. Yan, L. Hao, L. Xiaojun, and L. Liang, "Memory polynomial based adaptive predistortion for Radio over Fiber systems," in *International Conference on Microwave and Millimeter Wave Technology (ICMMT)*, 2012, pp. 1-4.

[27] M. Djamai, S. Bachir, and C. Duvanaud, "Kalman filtering algorithm for on-line memory polynomial predistortion," in *38th European Microwave Conference*, 2008, pp. 575-578.

[28] Y. Cuiping, F. Yongsheng, L. Yuanan, and X. Gang, "Memory polynomial digital predistortion for power amplifiers," in *International Symposium on Communications and Information Technologies ISCIT '07*, 2007, pp. 12-15.

[29] O. Hammi, F. M. Ghannouchi, and B. Vassilakis, "A Compact Envelope-Memory Polynomial for RF Transmitters Modeling With Application to Baseband and RF-

Digital Predistortion," *IEEE Transactions on Microwave and Wireless Components Letters,* vol. 18, pp. 359-361, 2008.

[30] P. Wensheng, L. Ying, and T. Youxi, "A Predistortion Algorithm Based on Accurately Solving the Reverse Function of Memory Polynomial Model," *IEEE Transactions on Wireless Communications Letters,* vol. 1, pp. 384-387, 2012.

[31] P. Varahram and Z. Atlasbaf, "Adaptive digital predistortion for high power amplifiers with memory effects," in *Asia-Pacific Conference Proceedings Microwave Conference Proceedings, APMC* 2005, p. 4 pp.

[32] O. Hammi, A. M. Kedir, and F. M. Ghannouchi, "Nonuniform memory polynomial behavioral model for wireless transmitters and power amplifiers," in *Asia-Pacific Microwave Conference Proceedings, APMC* 2012, pp. 836-838.

[33] Z. Hanxin, W. Guojin, and C. Limin, "A Nonlinear Memory Power Amplifier Behavior Modeling and Identification Based on Memory Polynomial Model in Soft-Defined Shortwave Transmitter," in *2010 6th International Conference on Wireless Communications Networking and Mobile Computing (WiCOM)* 2010, pp. 1-4.

[34] W. J. Jung, W. R. Kim, K. M. Kim, and K. B. Lee, "Digital predistorter using multiple lookup tables," *Electronics Letters,* vol. 39, pp. 1386–1388, 2003.

[35] P. Celka, N. J. Bershad, and J. Vesin, "Stochastic gradient identification of polynomial Wiener systems: analysis and application," *IEEE Transactions on Signal Processing,* vol. 49, pp. 301-313, 2001.

[36] A. E. Nordsjo and L. H. Zetterberg, "Identification of certain time-varying nonlinear Wiener and Hammerstein systems," *IEEE Transactions on Signal Processing,* vol. 49, pp. 577-592, 2001.

[37] K. Hyun-Woo, C. Yong-Soo, and Y. Dae-Hee, "Adaptive precompensation of Wiener systems," *IEEE Transactions on Signal Processing,* vol. 46, pp. 2825-2829, 1998.

[38] K. Hyun-Woo, C. Yong-Soo, and Y. Dae-Hee, "On compensating nonlinear distortions of an OFDM system using an efficient adaptive predistorter," *IEEE Transactions on Communications,* vol. 47, pp. 522-526, 1999.

[39] F. Taringou, O. Hammi, B. Srinivasan, R. Malhame, and F. M. Ghannouchi, "Behaviour modelling of wideband RF transmitters using Hammerstein–Wiener models," *IET Circuits Devices Syst,* vol. 4, pp. 282-290, 2010.

[40] O. Hammi, M. Younes, and F. M. Ghannouchi, "Metrics and Methods for Benchmarking of RF Transmitter Behavioral Models With Application to the Development of a Hybrid Memory Polynomial Model," *IEEE Transactions on Broadcasting,* vol. 56, pp. 350-357, 2010.

[41] L. Taijun, S. Boumaiza, and F. M. Ghannouchi, "Deembedding static nonlinearities and accurately identifying and modeling memory effects in wide-band RF transmitters," *IEEE Transactions on Microwave Theory and Techniques,* vol. 53, pp. 3578-3587, 2005.

[42] L. Taijun, S. Boumaiza, and F. M. Ghannouchi, "Augmented hammerstein predistorter for linearization of broad-band wireless transmitters," *IEEE Transactions on Microwave Theory and Techniques,* vol. 54, pp. 1340-1349, 2006.

[43]   M. Younes, O. Hammi, A. Kwan, and F. M. Ghannouchi, "An Accurate Complexity-Reduced “PLUME” Model for Behavioral Modeling and Digital Predistortion of RF Power Amplifiers," *IEEE Transactions on Industrial Electronics,* vol. 58, pp. 1397-1405, 2011.

[44]   S. Haykin, "Neural Networks: a comprehensive foundation," *Prentice Hall,* 1999.

[45]   F. H. Raab, P. Asbeck, S. Cripps, P. B. Kenington, Z. B. Popovic, N. Pothecary, J. F. Sevic, and N. O. Sokal, "Power amplifiers and transmitters for RF and microwave," *IEEE Transactions on Microwave Theory and Techniques,* vol. 50, pp. 814-826, 2002.

[46]   M. Allegue-Martinez, M. J. Madero-Ayora, J. Reina-Tosina, J. Navarro-Lazaro, and C. Crespo-Cadenas, "Low frequency nonlinear memory effects in M-ary QAM communications systems," *Microw. Opt. Technol. Lett,* vol. 3 pp. 826–829, 2012.

[47]   C. Jebali, Boulejfen, N., Rawat, M., Gharsallah, A., Ghannouchi, F.M, "Modeling of wideband radio frequency power amplifiers using Zernike polynomials," *International Journal of RF and Microwave Computer-Aided Engineering,* vol. 3, pp. 289–296 2012.

[48]   A. Zhu, J. C. Pedro, and T. R. Cunha, "Pruning the Volterra Series for Behavioral Modeling of Power Amplifiers Using Physical Knowledge," *IEEE Transactions on Microwave Theory and Techniques,* vol. 55, pp. 813-821, 2007.

[49]   A. Kwan, F. M. Ghannouchi, O. Hammi, M. Helaoui, and M. R. Smith, "Look-up table-based digital predistorter implementation for field programmable gate arrays using long-term evolution signals with 60 mhz bandwidth," *Science, Measurement & Technology, IET,* vol. 6, pp. 181-188, 2012.

[50]   J. Weston, A. Ellisseeff, B. Scholkopf, and M. Tipping, "Use of the zero-norm with linear models and kernel methods," *Journal of Machine Learning Research,* vol. 3, pp. 1439–1461 2003.

[51]   X. Hong, S. Chen, and C. J. Harris, "Using zero-norm constraint for sparse probability density function estimation," *International Journal Systems Science,* vol. 43, pp. 2107–2113 2012.

[52]   J. Sung-chan, O. Hammi, and F. M. Ghannouchi, "Design Optimization and DPD Linearization of GaN-Based Unsymmetrical Doherty Power Amplifiers for 3G Multicarrier Applications," *IEEE Transactions on Microwave Theory and Techniques,* vol. 57, pp. 2105-2113, 2009.

[53]   O. Hammi, A. Kwan, and F. M. Ghannouchi, "Bandwidth and Power Scalable Digital Predistorter for Compensating Dynamic Distortions in RF Power Amplifiers," *IEEE Transactions on Broadcasting,* vol. PP, pp. 1-1, 2013.

[54]   T. Soderstrom and P. Stoica, "System Identification," *Prentice Hall,* 1989.

[55]   L. Ljung, "System Identification, Theory for the user," *Prentice Hall,* 1999.

[56]   J. Moon and B. Kim, "Enhanced Hammerstein behavioral model for broadband wireless transmitters," *IEEE Trans. Microw. Theory Tech,* vol. 59, pp. 924-933, 2011.

[57]   J. Kim and K. Konstantinou, "Digital predistortion of wideband signals based on power amplifier model with memory," *IEE Electronic Letters,* vol. 23, pp. 1417-1418, 2001.

[58] O. Hammi, F. M. Ghannouchi, S. Boumaiza, and B. Vassilakis, "A data-based nested LUT model for RF power amplifiers exhibiting memory effects," *IEEE Microw. Wireless Compon. Lett,* vol. 17, pp. 712-714, 2007.

[59] O. Hammi, S. Carichner, B. Vassilakis, and F. M. Ghannouchi, "Power amplifiers' model assessment and memory effects intensity quantification using memoryless post-compensation technique," *IEEE Trans. Microw. Theory Tech,* vol. 56, pp. 3170-3179, 2008.

[60] A. Kwan, O. Hammi, M. Helaoui, and F. M. Ghannouchi, "High performance wideband digital predistortion platform for 3G+ applications with better than 55dBc over 40 MHz bandwidth," *IEEE MTT-S International Microwave Symposium,* vol. IMS'2010, , pp. 1082-1085, 2010.

[61] F. M. Ghannouchi, F. Taringou, and O. Hammi, "A dual branch Hammerstein-Wiener architecture for behavior modeling of wideband RF transmitters," in *IEEE MTT-S International Microwave Symposium Digest (MTT),* , 2010, pp. 1692-1695.

[62] F. M. Ghannouchi, M. Younes, and M. Rawat, "Distortion and impairments mitigation and compensation of single- and multi-band wireless transmitters (invited)," *Microwaves, Antennas & Propagation, IET,* vol. 7, pp. 518-534, 2013.

[63] P. Crama and Y. Rolain, "Broadband measurement and identification of a Wiener-Hammerstein model for an RF amplifier," *ARFTG Conference Digest,* vol. 60, pp. 49 - 57, 2002.

[64] O. Hammi, S. Carichner, B. Vassilakis, and F. M. Ghannouchi, "Novel approach for static nonlinear behavior identification in RF power amplifiers exhibiting memory effects," in *IEEE MTT-S International Microwave Symposium Digest*, 2008, pp. 1521-1524.

Vitae

Name   :Abderezak Miftah Kedir

Nationality   :Ethiopian

Date of Birth   :10/22/1984

Email   :abderezakmiftah@gmail.com; g201102730@kfupm.edu.sa

Address   :Kolfe Keranio, HN607, K12, Addis Ababa, Ethiopia

Academic Background   :BSc in Electrical Engineering from Hawassa

University,2007, Ethiopia, graduated with "great distinction" , ranked 2nd from

Faculty of Technology.

Completed trainings in BSS, wireless network planning & optimization from ZTE

University; 2008, Ethiopia

Completed training on railway signaling & automation, 2010, China organized by

China Railway Signal & Communication Shanghai Engineering Co.

Work Experience

1. Research Assistant, 2011 to 2013, CCITR, KFUPM, RI, Saudi Arabia

2. BSS P&D Technical Manager, 2010 to 2011, ZTE (H.K) ltd Ethiopian Branch

3. RF Planning & Optimization Senior Engineer 2008 to 2010 ZTE (H.K) ltd

4. RF Planning & Optimization Junior Engineer, 2007 to 2008 ZTE (H.K) ltd